Supplementary Materials: Climate refugia for Asian elephants in Bhutan lie largely outside the protected-area network

Supplementary Appendices S1-S5 | Supplementary Figures S1-S21 | Supplementary Tables S1-S18

Supplementary Appendix S1: ODMAP Protocol Compliance

Standard protocol for reporting species distribution models (Zurell et al., 2020).

O – Overview

Item	Description
Modelling objective	To infer environmental drivers of habitat suitability and project future distributions under climate change scenarios.
Target entity	*Elephas maximus* Linnaeus, 1758.
Scale of analysis	National extent (Bhutan; 32,973 km²).
Projection extent	Equivalent to the calibration extent.
Study period	Present: 1986–2015 baseline; Future: 2021–2100 (three 30-year periods).
Biodiversity data type	Empirical presence–absence survey data.
Conceptual model	Habitat suitability is modelled as a function of climatic, topographic, vegetation, and anthropogenic-distance predictors.
SDM context	Temporal transferability and conservation-oriented spatial prediction.

D - Data

Occurrence data: Occurrence records were derived from the national elephant and tiger survey, implemented through a systematic camera-trap network across Bhutan. Sampling followed an approximately 5 × 5 km grid, yielding near-complete national coverage. The operational occurrence dataset comprised 1,089 station-level records. Coordinate quality control and exact-coordinate deduplication were applied separately to presence and absence observations, resulting in 252 verified presences and 837 verified absences. No pseudo-absences were generated, and no additional spatial thinning was applied. Presence records were spatially concentrated in the southern lowlands, with 63.5% located within the protected-area network.

Environmental predictors: An initial set of 35 candidate predictors was evaluated. Collinearity screening ($|r| < 0.85$; VIF < 10) reduced this to 17 retained variables, including: BIO05, BIO14, BIO15, BIO18, terrain ruggedness index (TRI), slope, aspect, human footprint, enhanced vegetation index (EVI), Dynamic World probability and land-cover class, and distances to major rivers, streams, water sources, settlements, protected areas, and private land.

Future climate data: All 96 CMIP6 scenarios were implemented, comprising 8 GCMs, four SSPs, and three future periods. Climatic predictors were projected under future scenarios, whereas non-climatic predictors were held constant at present-day conditions. Future SSP–period projection surfaces were derived as simple arithmetic means across the 8 GCMs. GCM reliability scores were computed and retained as diagnostic metrics to characterise inter-model behaviour, but they were not used as weighting factors in ensemble construction.

M - Model

Algorithms: Generalised Linear Models (GLM), Random Forest (RF), Boosted Regression Trees (BRT), and MaxEnt were implemented.

Model complexity:

- GLM: forward stepwise selection using AIC
- RF: 1,000 trees; *mtry* = 4
- BRT: 1,000 trees; tree depth = 3; learning rate = 0.01; bag fraction = 0.75
- MaxEnt: regularisation multiplier = 1.5; feature classes = hinge, product, linear, quadratic

Spatial cross-validation: Five-fold spatial blocking using 15 km blocks (seed = 123458) to minimise spatial autocorrelation.

Ensemble method: Present-day ensemble suitability was computed as an AUC-weighted mean across the four algorithms. Future SSP–period projections were calculated as simple arithmetic means across the 8 GCMs.

Threshold: A threshold of 0.174 (rounded ensemble threshold) was applied consistently for binary classification.

Null model testing: Statistical significance was evaluated using 99 label-permuted null models per algorithm. All empirical models performed significantly better than null expectations ($p < 0.010$).

A - Assessment

Extrapolation analysis: Multivariate Environmental Similarity Surface (MESS) analyses were conducted for each GCM–scenario combination. The mean extrapolation fraction across SSP-period combinations was 0.001260 (0.13% of pixels), with a maximum of 0.001965 (0.20%) under SSP3–7.0 (2051–2080).

Scenario coverage: All 96 target scenarios were successfully completed.

GCM reliability: Composite reliability scores ranged from 0.000 to 0.840. These values were used diagnostically to identify outlier model behaviour and were not incorporated into ensemble weighting.

P - Prediction

Present-day suitability: The ensemble model identified 4,670 km² (14.2% of Bhutan) as suitable habitat at the selected threshold (0.174).

Future projections: Across SSP-period mean projections, suitable habitat ranged from 4,377 km² (−6.3%) to 5,558 km² (+19.0%) relative to present conditions.

Climate refugia: Core refugia encompassed 4,160 km² (12.6% of Bhutan), of which 46.4% occurred within the protected-area network. This indicates that a substantial proportion of climatically stable habitat lies outside formally protected areas.

Supplementary Appendix S2: Predictor Processing Details

Climate Predictors (CMIP6-based Bhutan 250 m dataset)

Bioclimatic variables (BIO01–BIO19) were obtained from CMIP6-based high-resolution (~250 m) climate datasets developed for Bhutan (Dorji et al., 2025), representing 30-year climatological normal for the 1986–2015 reference period. These datasets are derived from monthly temperature and precipitation outputs of multiple general circulation models and downscaled to account for complex topographic and orographic effects characteristic of the Himalayan region. Four bioclimatic variables were retained after collinearity screening: BIO05 (maximum temperature of the warmest month), BIO14 (precipitation of the driest month), BIO15 (precipitation seasonality — coefficient of variation), and BIO18 (precipitation of the warmest quarter). All retained bioclimatic variables are expressed in standard WorldClim units (temperature: °C × 10 stored as integer and converted to °C for analysis; precipitation: mm).

Future bioclimatic variables were derived from the same CMIP6 framework for 96 scenarios (8 general circulation models × 4 shared socioeconomic pathways × 3 time periods), ensuring consistency between baseline and projected climate layers.

Digital Elevation Model and Topographic Derivatives

Topographic predictors were derived from a high-resolution (12.5 m) digital elevation model (TanDEM-X/ALOS). Slope, aspect, and terrain ruggedness index (TRI; Wilson et al., 2007) were computed using *terra::terrain()* and subsequently resampled to the 250 m analysis grid using bilinear interpolation. Elevation was excluded from modelling due to strong collinearity with BIO05 ($r = -0.98$), indicating that thermal gradients effectively capture elevational variation in this system.

Vegetation Indices (MOD13Q1)

Annual mean EVI and NDVI were computed as pixel-wise means across all annual composite layers of the MODIS MOD13Q1 product (250 m, 16-day composites, 2000–2024), quality-filtered using the companion QA layer. NDVI was excluded due to collinearity with Dynamic World probability ($r = 0.86$). EVI was retained as an independent measure of vegetation productivity less saturated than NDVI in dense canopy conditions.

Dynamic World Land Cover (Brown et al., 2022)

A 2025 annual composite of Google Dynamic World (10 m; Brown et al., 2022) was used to derive two predictors: (1) the probability of the dominant land-cover class (a continuous [0,1] measure of land-cover confidence, hereafter “DW probability”) and (2) the integer land-cover class code. Both layers were resampled to 250 m using nearest-neighbour (class) and bilinear (probability) interpolation.

Human Influence Index (HII)

The Human Influence Index (version 2020 update; Wildlife Conservation Society/CIESIN, 2005) was used as a measure of cumulative anthropogenic modification of the landscape, incorporating human population density, land transformation, human access, and electrical infrastructure. The HII was resampled to 250 m using bilinear interpolation.

Distance Layers

Euclidean distance layers were generated with terra::distance() from national GIS vector datasets representing major rivers, streams above order 3, water sources, building footprints used as settlement proxies, protected-area boundaries, and private cadastral land boundaries.

Spatial Alignment

Bioclimatic predictor layers were supplied in a non-standard transverse Mercator projection with a central meridian of 90°E. Before analysis, these layers were explicitly reprojected to EPSG:32645 (WGS 84 / UTM Zone 45N). All predictor layers were then projected, resampled, and aligned to a common 250 m grid defined from the national Bhutan boundary (bhutan.shp). Continuous variables were resampled using bilinear interpolation, whereas categorical variables were resampled using nearest-neighbour assignment in terra::project().

Supplementary Appendix S3: GCM Selection, Reliability, and Outlier Assessment

GCM selection rationale

Eight CMIP6 general circulation models were retained: ACCESS-CM2, CNRM-CM6-1, CNRM-ESM2-1, INM-CM4-8, INM-CM5-0, MIROC6, MPI-ESM1-2-LR, and MRI-ESM2-0. These models were consistently implemented across all SSPs and time periods to maintain comparability across the full scenario ensemble.

GCM reliability scoring

The diagnostic ranking combined two quantities: (1) the mean intra-algorithm SD of each GCM's future projections and (2) the mean absolute deviation of each GCM from the SSP-period ensemble mean. These components were normalised to [0,1] and combined into a composite reliability score. Higher scores indicate closer agreement with the ensemble and lower internal variability. INM-CM5-0 ranked highest (0.840), followed by CNRM-CM6-1 (0.804) and MIROC6 (0.796); MRI-ESM2-0 ranked lowest (0.000).

Interpretation of outliers

ACCESS-CM2 and MRI-ESM2-0 projected larger suitable areas than the central cluster of GCMs and were therefore identified as diagnostic outliers. However, all 8 GCMs were retained to preserve the full uncertainty envelope represented by the CMIP6 ensemble. Future SSP–period projections were calculated as simple arithmetic means across GCMs. Reliability scores were used only to describe inter-model behaviour and were not applied as ensemble weights.

Supplementary Appendix S4: Supplementary Figures

Figure S1. Algorithm-specific present-day habitat suitability maps for *Elephas maximus* in Bhutan. Continuous suitability predictions from each of the four modelling algorithms: (a) Generalised Linear Model (GLM), (b) Random Forest (RF), (c) Boosted Regression Trees (BRT), and (d) Maximum Entropy (MaxEnt), evaluated on full-model predictions using the 1986–2015 climate baseline. All algorithms predict concentrated habitat in the subtropical southern belt; RF and MaxEnt show sharper suitability gradients.

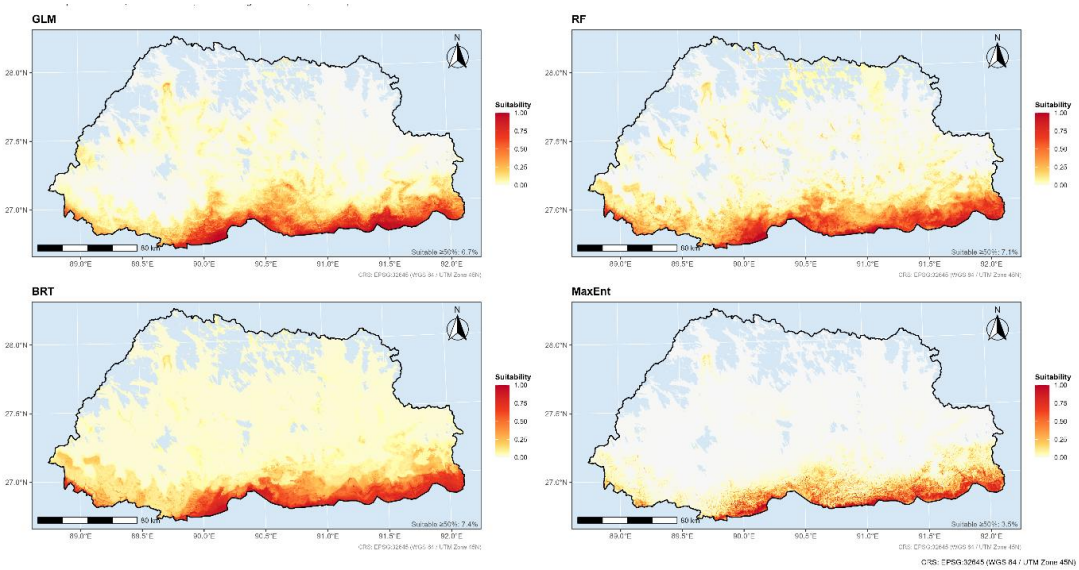

Figure S2. Receiver operating characteristic (ROC) curves for all four algorithms. ROC curves derived from out-of-fold predicted probabilities aggregated across five spatial folds. Fold-level AUC means +/- SD were GLM = 0.923 +/- 0.035, RF = 0.948 +/- 0.037, BRT = 0.943 +/- 0.042, and MaxEnt = 0.949 +/- 0.037. The diagonal dashed line indicates null expectation.

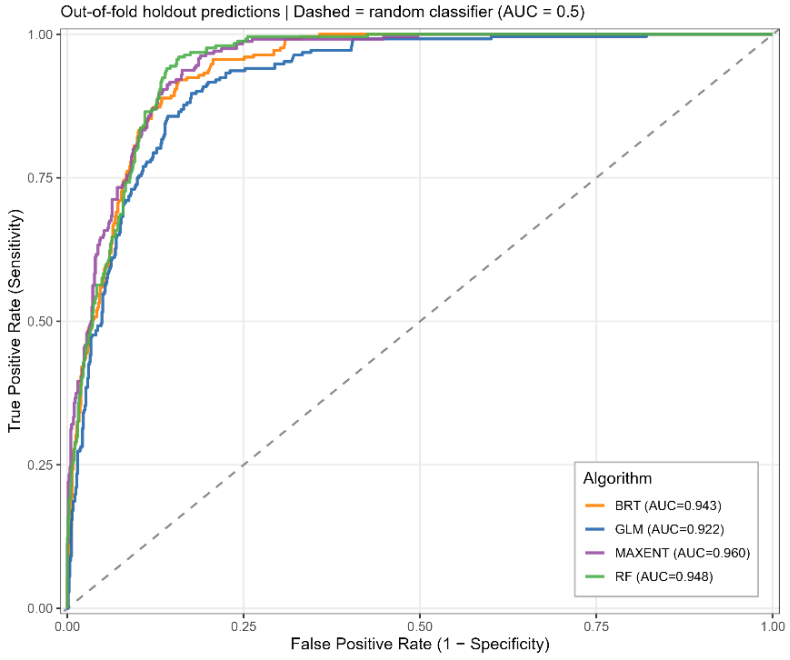

Figure S3. Calibration plots for all four algorithms. Observed presence rate (binned) versus predicted probability, derived from OOF predictions. Perfect calibration corresponds to the 1:1 diagonal. GLM (calibration slope = 0.846) shows slight under-dispersion; RF (1.292) and BRT (1.279) show slight over-dispersion; MaxEnt (0.935) is closest to ideal calibration.

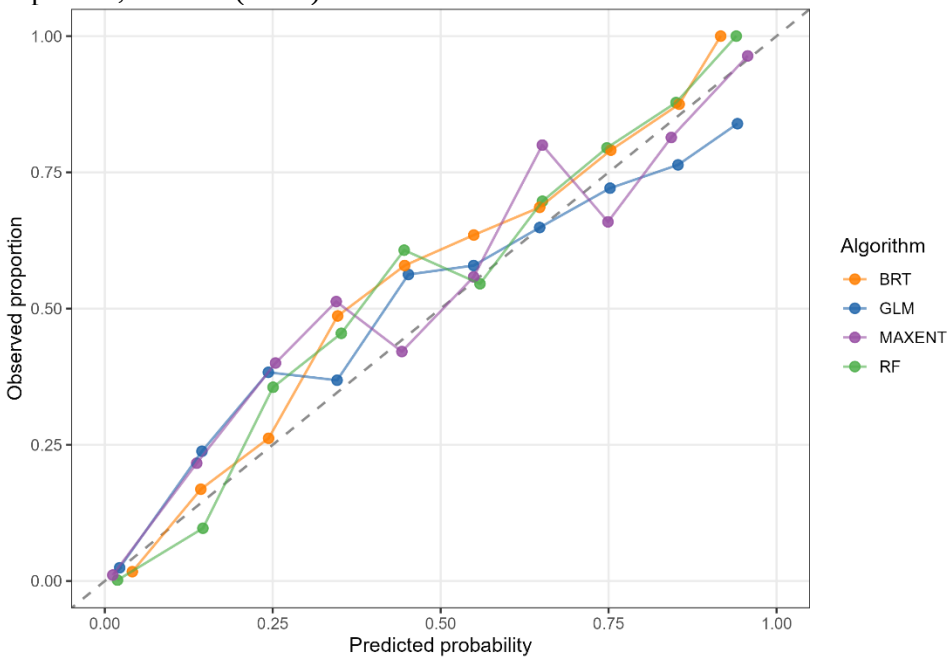

Figure S4. Null model comparison — observed AUC versus permuted null distribution. Distribution of AUC values from 99 label-permuted null models (grey histograms) for each algorithm, with observed OOF AUC shown as a vertical red line. All observed AUC values exceed the 99th percentile of their null distributions (empirical p < 0.010 for all algorithms).

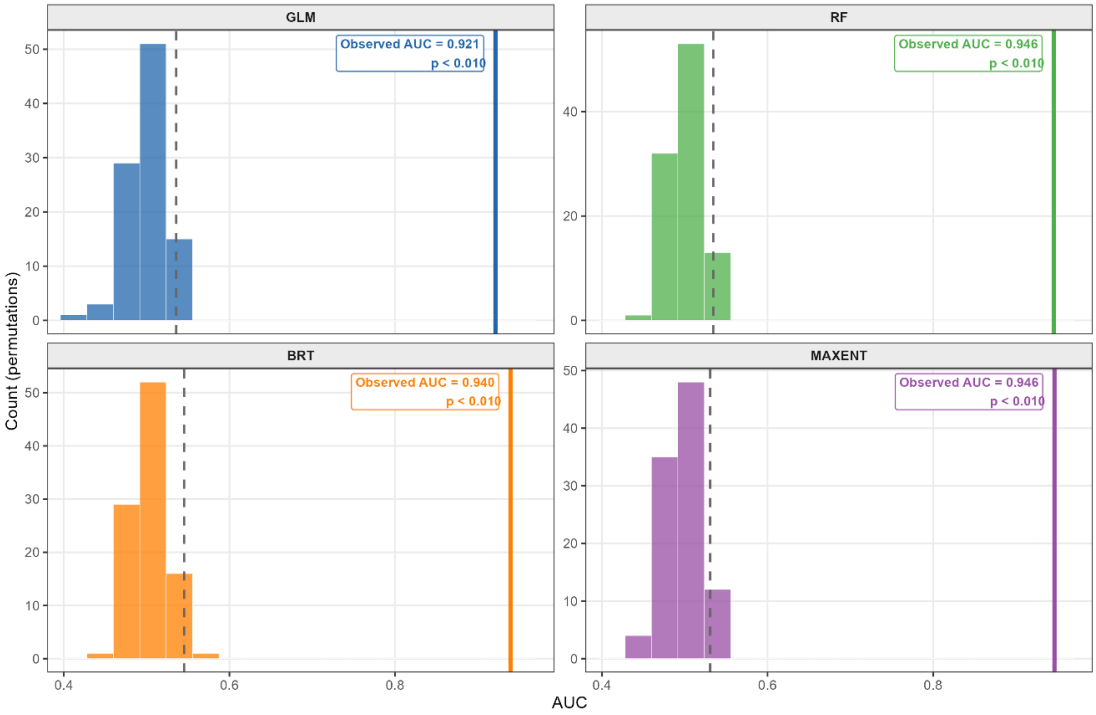

Figure S5. Spatial cross-validation fold performance. (a) Per-fold AUC for each algorithm across five spatially blocked folds. (b) Fold composition: number of presence records per fold (range: 19–80) and presence: absence balance ratio. Fold 1 is the smallest (19 presences; balance = 0.12), contributing wider confidence intervals; fold 4 is the most balanced (80 presences; balance = 0.50).

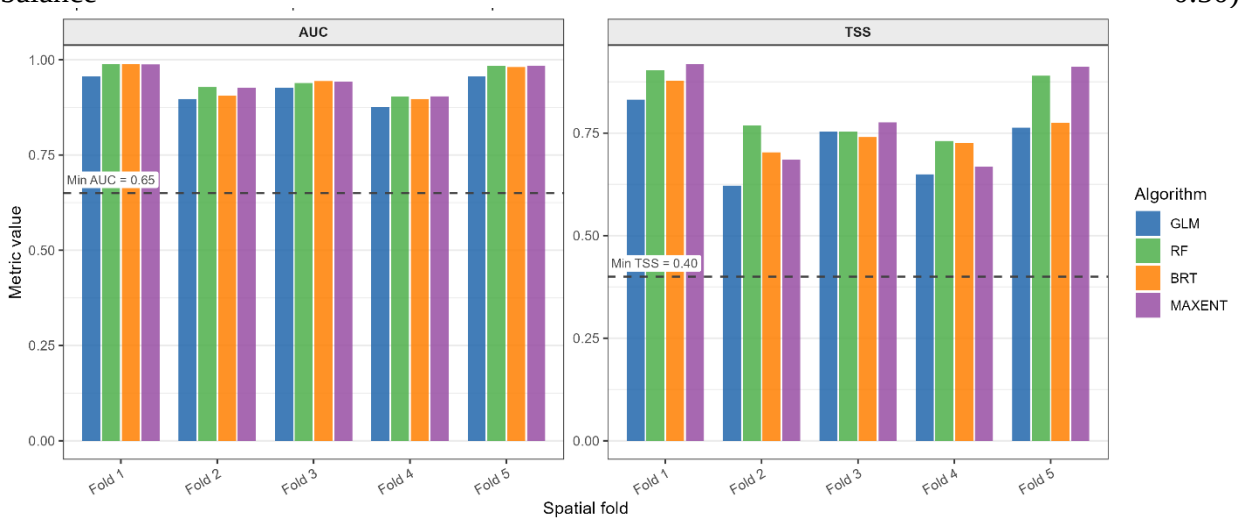

Figure S6. Predictor collinearity matrix — all 35 candidate predictors. Pairwise Pearson correlation matrix for the 35 candidate predictors evaluated on the combined presence and absence dataset. Cells exceeding |r| = 0.85 triggered removal of the less defensible predictor, and VIF screening removed an additional four variables. The predictor-selection workflow excluded 18 predictors in total, leaving 17 retained predictors for modelling.

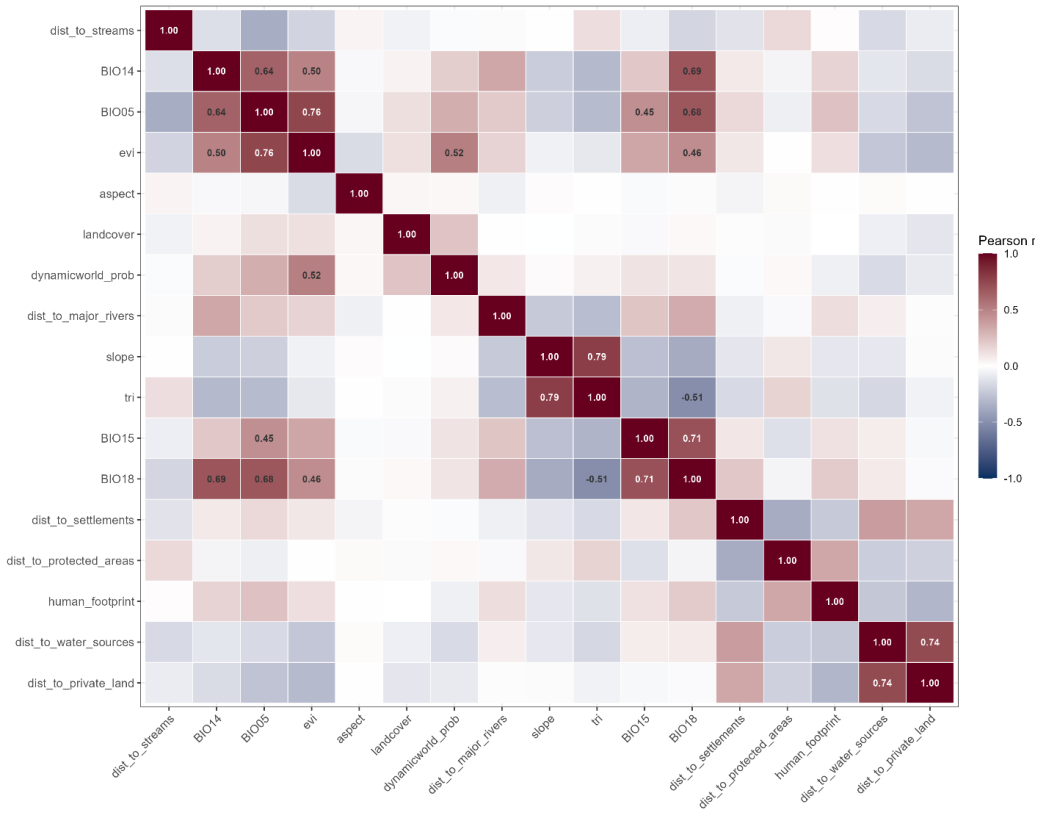

Figure S7. Threshold sensitivity analysis. Habitat area classified as suitable (km² and % of Bhutan) as a function of ensemble suitability threshold, ranging from 0.05 to 0.50. The TSS-maximising threshold used in the main analysis (0.174) is indicated. Habitat area ranges from 9,439 km² at threshold = 0.05 to 1,938 km² at threshold = 0.50, underscoring the sensitivity of binary classification to threshold choice.

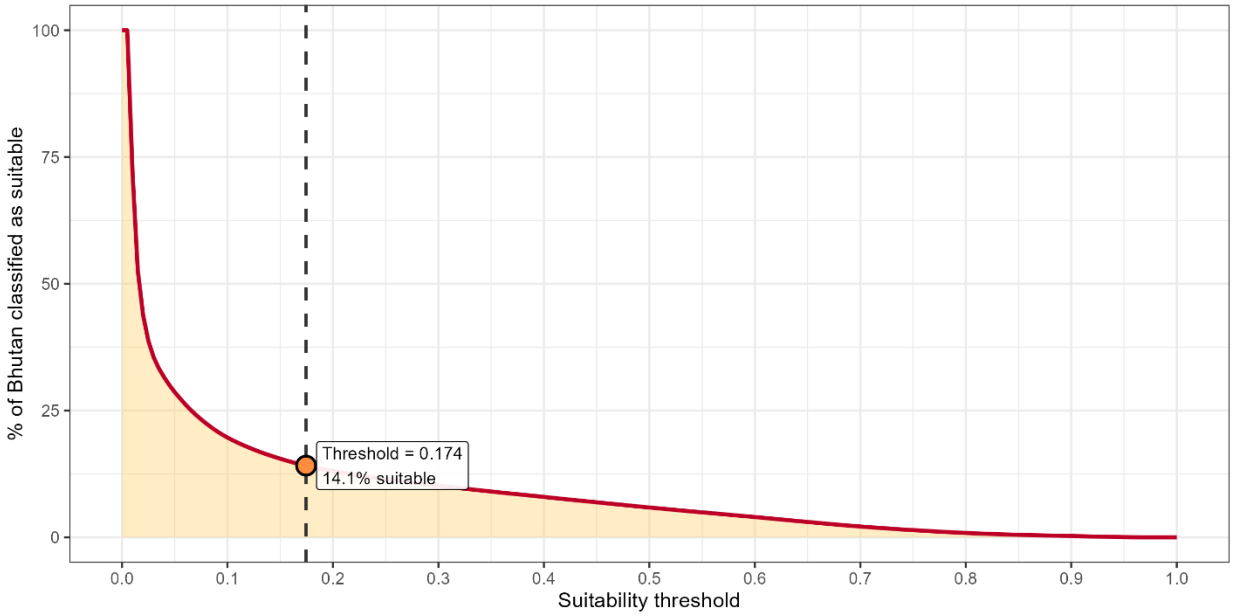

Figure S8. Climate envelope analysis. (a) Principal component analysis (PCA) biplot of 1986–2015 calibration climate space (grey points = background; coloured points = presence stations), showing the occupation of a distinct warm-wet climate niche. (b) Climate PCA biplot with future GCM scenario centroids overlaid, illustrating the direction and magnitude of projected climate change relative to the calibration space. Most future scenarios remain within the calibration envelope.

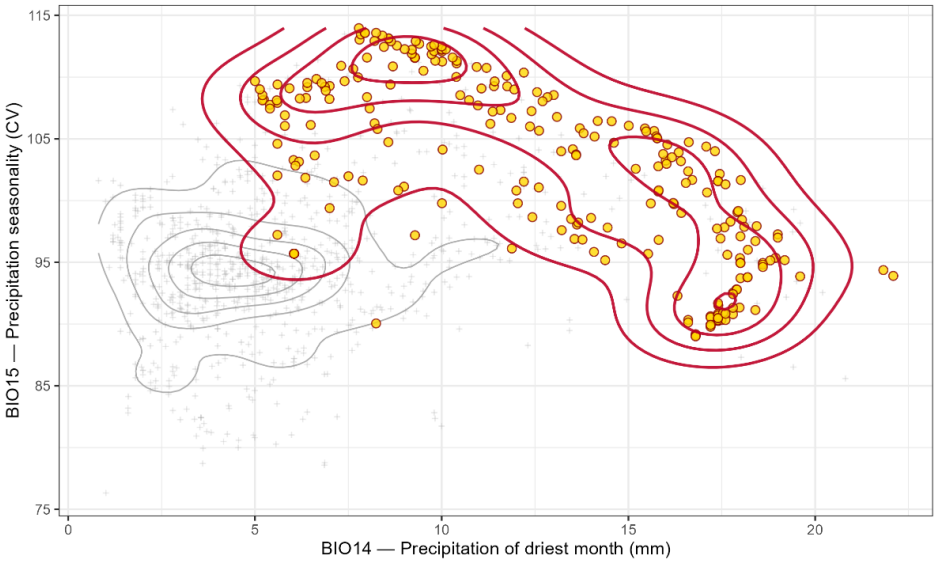

Figure S8a. Climate envelope PCA biplot.

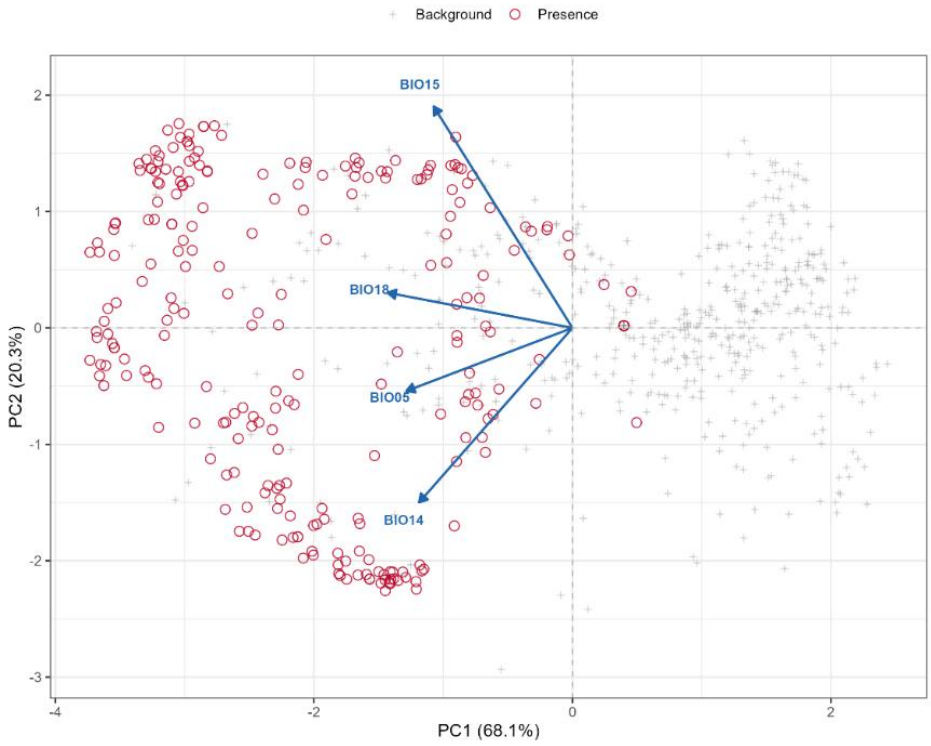

Figure S8b. Climate PCA biplot with future GCM centroids.

Figure S9. Full marginal response curves — all 17 predictors × 4 algorithms. Marginal response of ensemble suitability (mean ± 95% CI across cross-validation folds) to each of the 17 retained predictors, shown separately for GLM (black), RF (blue), BRT (green), and MaxEnt (red). Predictor values on the x-axis span the range observed in the combined presence-absence dataset.

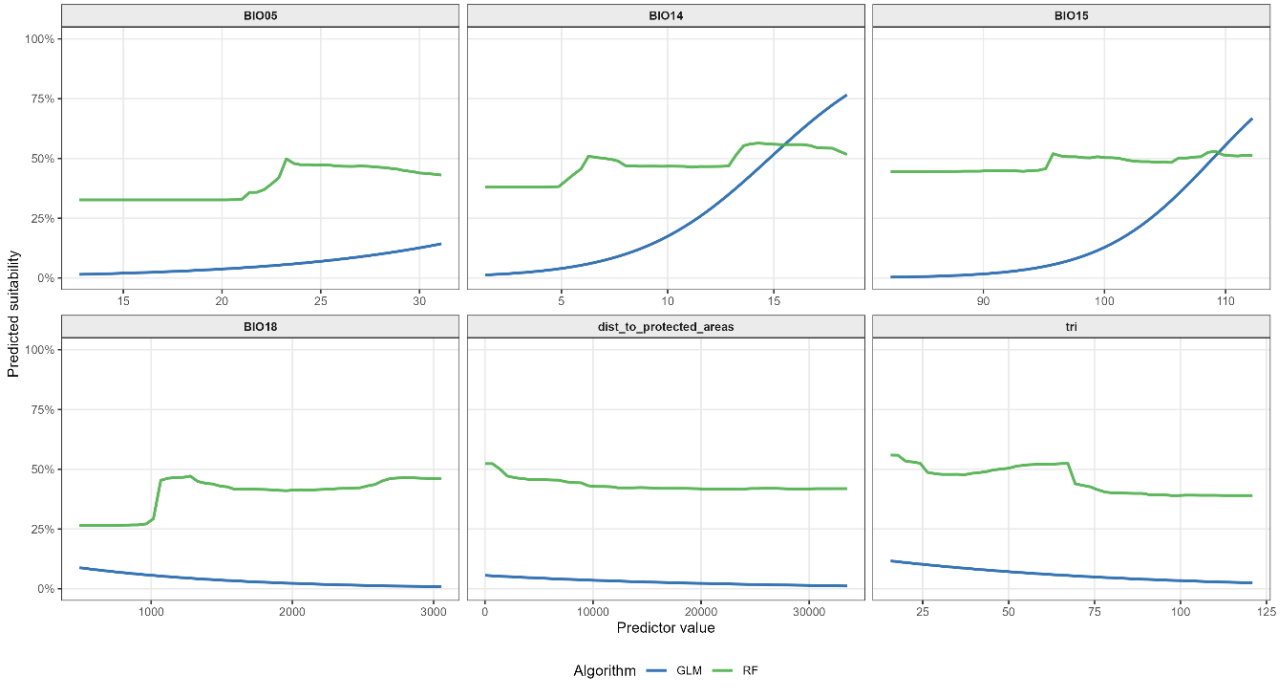

Figure S10. Occurrence and absence data spatial distribution. (a) Spatial distribution of the 252 presence records (filled circles) and 837 absence stations (open circles) across Bhutan, overlaid on a continuous elevation map. Station density is highest in the southern lowland Dzongkhags and within the PA network, reflecting the distribution of survey effort. (b) Kernel density surface of presence records, showing highest detection probability in Samdrup Jongkhar, Pemagatshel, and Sarpang.

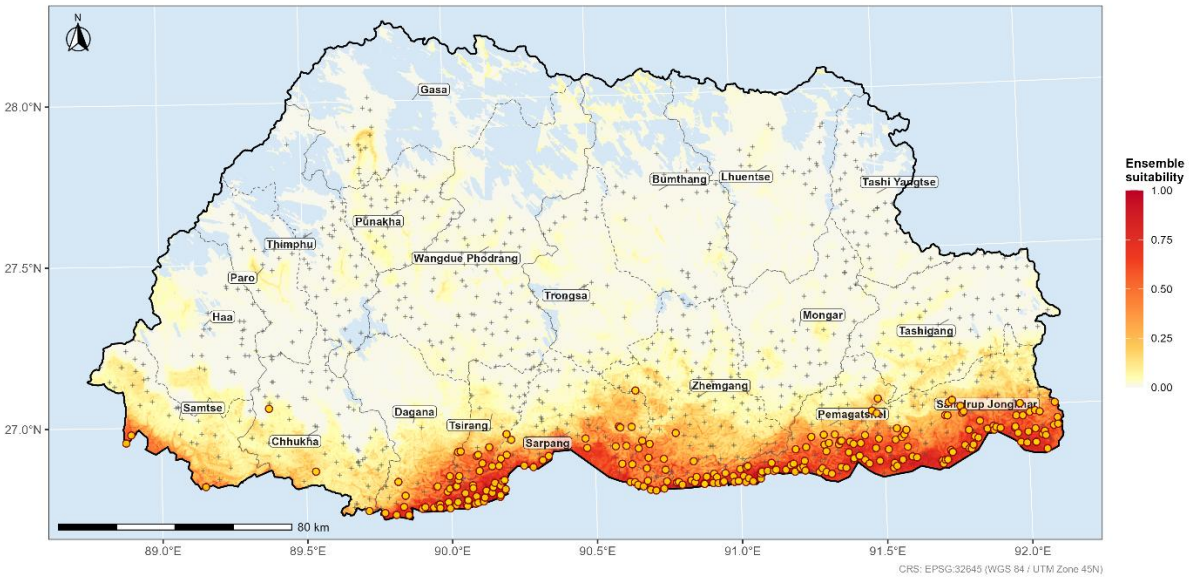

Figure S10a. Occurrence and absence spatial distribution.

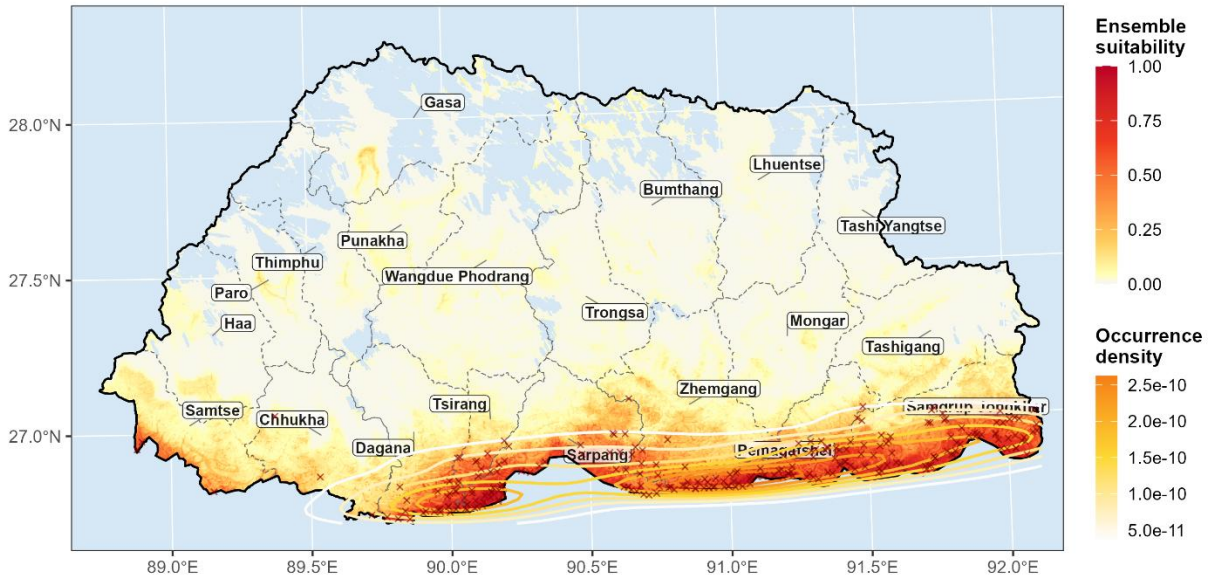

Figure S10b. Kernel density of presence records.

Figure S11. Inter-GCM agreement maps. Proportion of the 8 GCMs predicting suitable habitat (binary, at the ensemble threshold) for each of the 12 future SSP × period combinations. High agreement (>75% GCMs agree) is shown in dark colours; low agreement in light colours. Areas of persistent inter-GCM disagreement coincide with the habitat gain/loss margins at higher elevations.

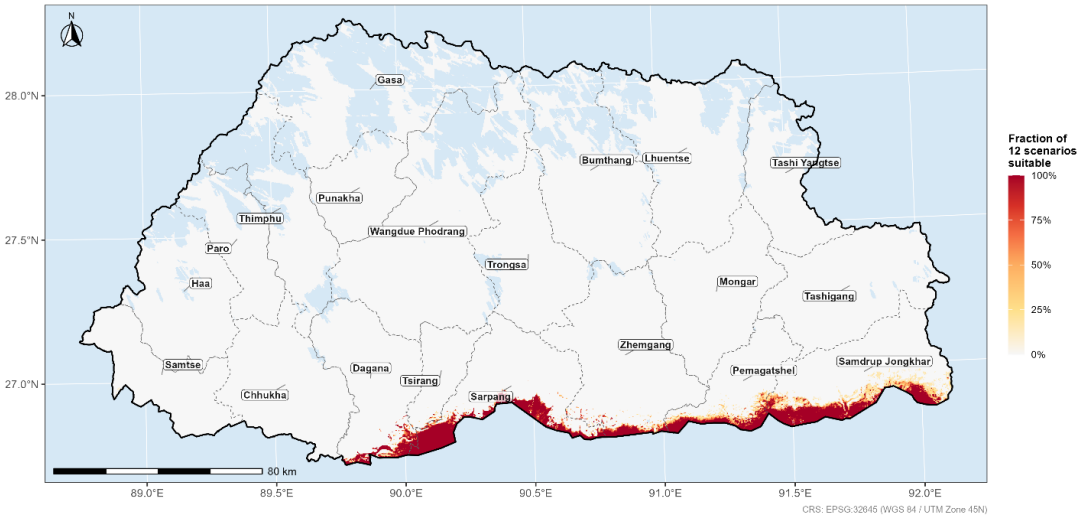

Figure S12. Inter-GCM spread maps. Standard deviation of continuous suitability scores across the 8 GCMs for each of the 12 future scenarios. Uncertainty is highest at range margins (particularly the submontane zone at 800–1,500 m elevation) and under SSP5-8.5 by 2071–2100 (mean SD = 0.042; 11.3% of pixels with high SD). Core lowland habitat shows consistently low inter-GCM spread.

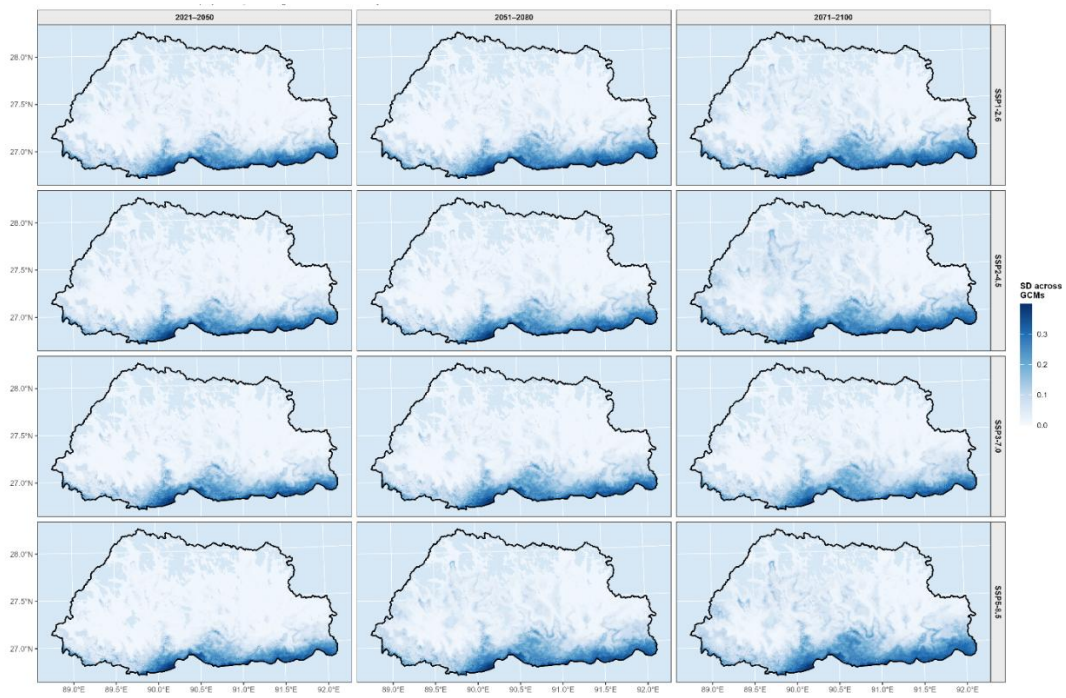

Figure S13. GCM reliability ranking. Composite reliability scores for all 8 GCMs (see Appendix S3 for methodology). Bars are coloured by score: dark green = higher diagnostic reliability (INM-CM5-0: 0.840, CNRM-CM6-1: 0.804, MIROC6: 0.796); orange = moderate; red = lower diagnostic reliability (ACCESS-CM2: 0.356, MRI-ESM2-0: 0.000). These scores were used to rank GCM behaviour and were not used to weight the future SSP–period projections.

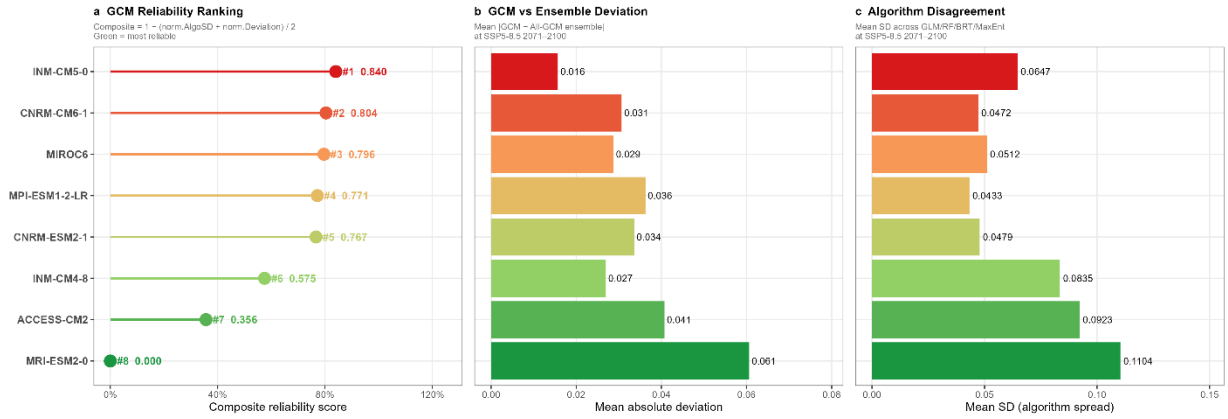

Figure S14. Individual GCM habitat area trajectories. Habitat area (km2) projected by each of the 8 GCMs individually across 4 SSPs and 3 time periods. ACCESS-CM2 and MRI-ESM2-0 are the clearest outliers relative to the tighter central cluster of GCMs. The coloured line represents the simple across-GCM mean for each SSP-period combination, and the grey ribbon shows the full GCM range.

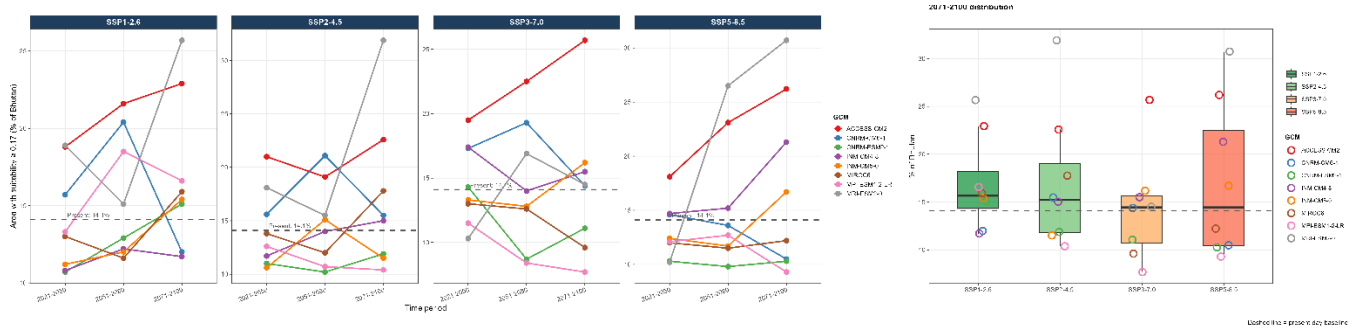

Figure S15. Future ensemble habitat suitability for Elephas maximus in Bhutan, derived by projecting the AUC-weighted multi-algorithm ensemble onto CMIP6 climate data and calculating the simple arithmetic mean across 8 GCMs for each SSP–period combination. Panels show (a) 2021–2050, (b) 2051–2080, and (c) 2071–2100. High suitability remains concentrated in the southern subtropical belt, with expansion into submontane zones in later periods.

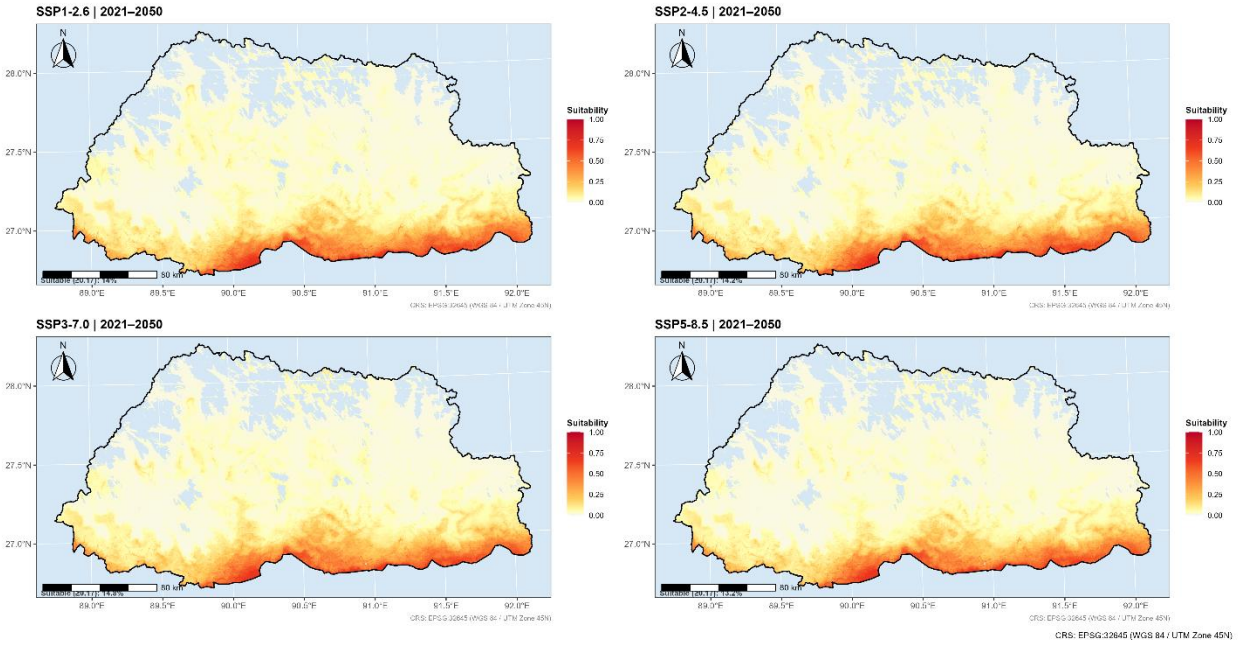

Figure S15a. Future ensemble suitability 2021–2050.

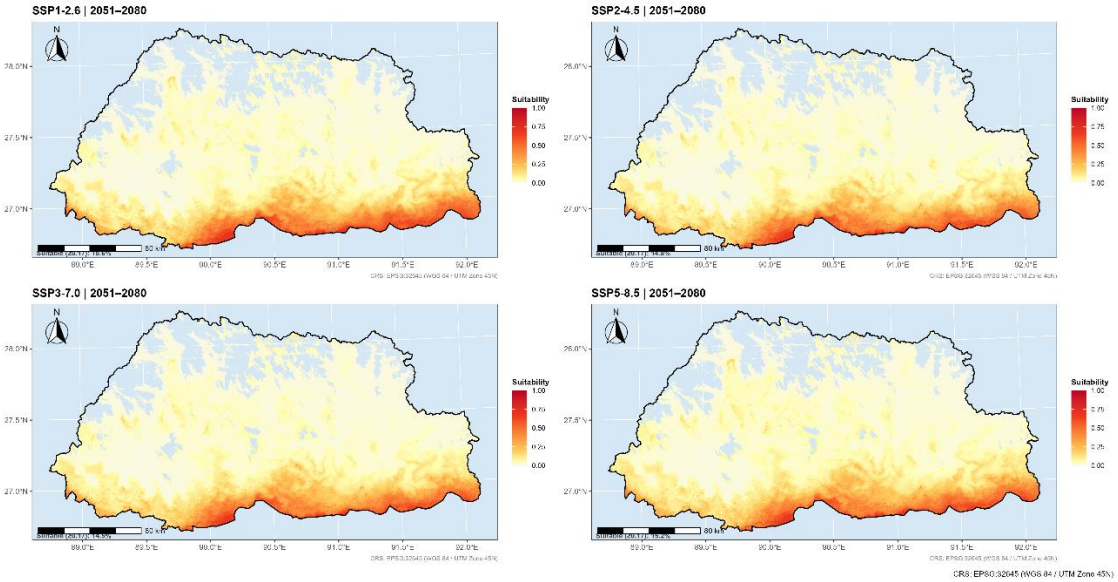

Figure S15b. Future ensemble suitability 2051–2080.

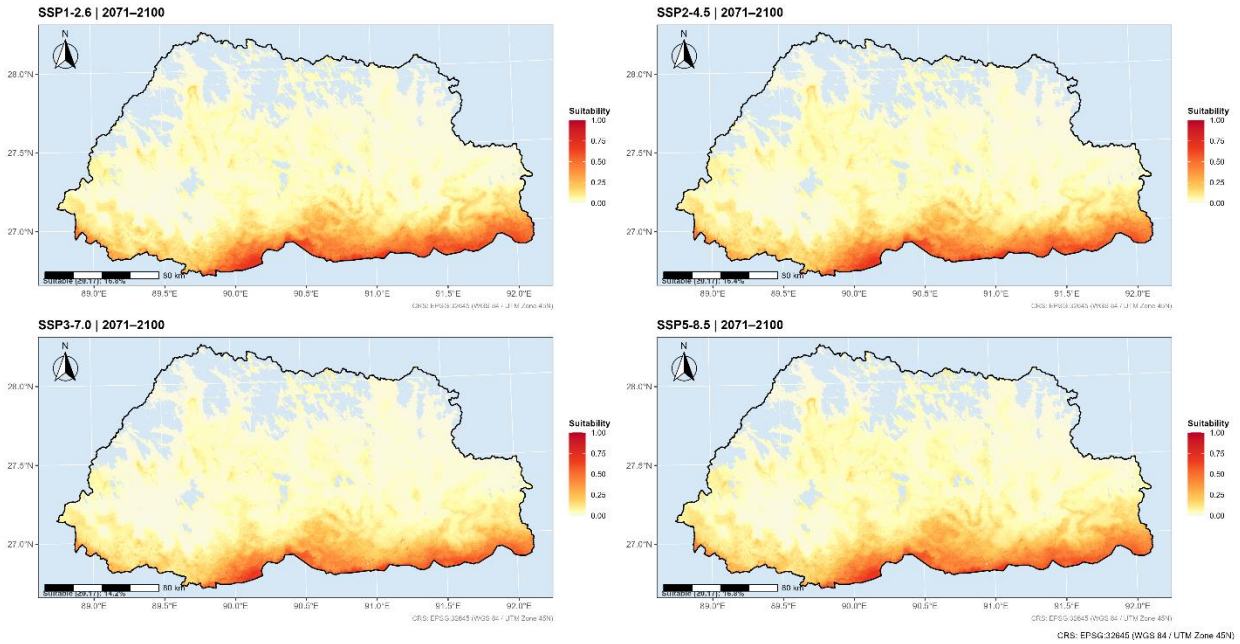

Figure S15c. Future ensemble suitability 2071–2100.

Figure S16. Habitat change maps by time period (all scenarios). Binary habitat change maps (suitable vs. not suitable relative to present-day baseline) for 2021–2050, 2051–2080, and 2071–2100, aggregated across SSPs showing dominant change category (gain, loss, no-change, persistence).

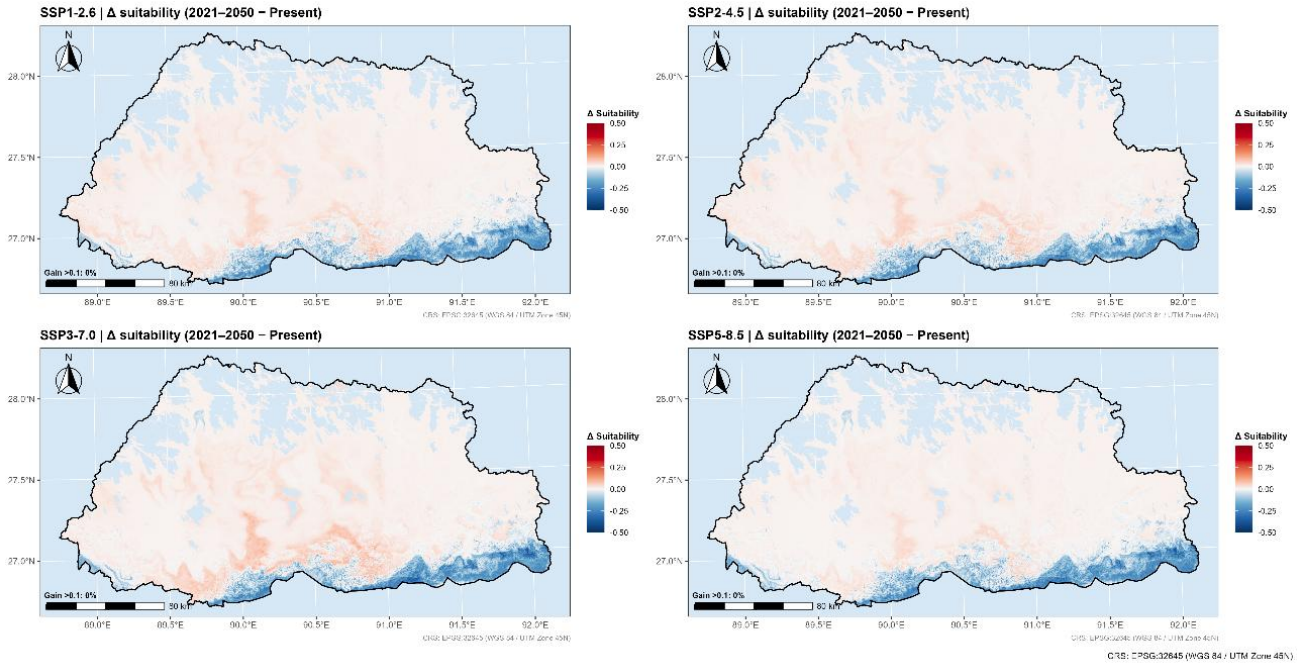

Figure S16a. Habitat change map 2021–2050.

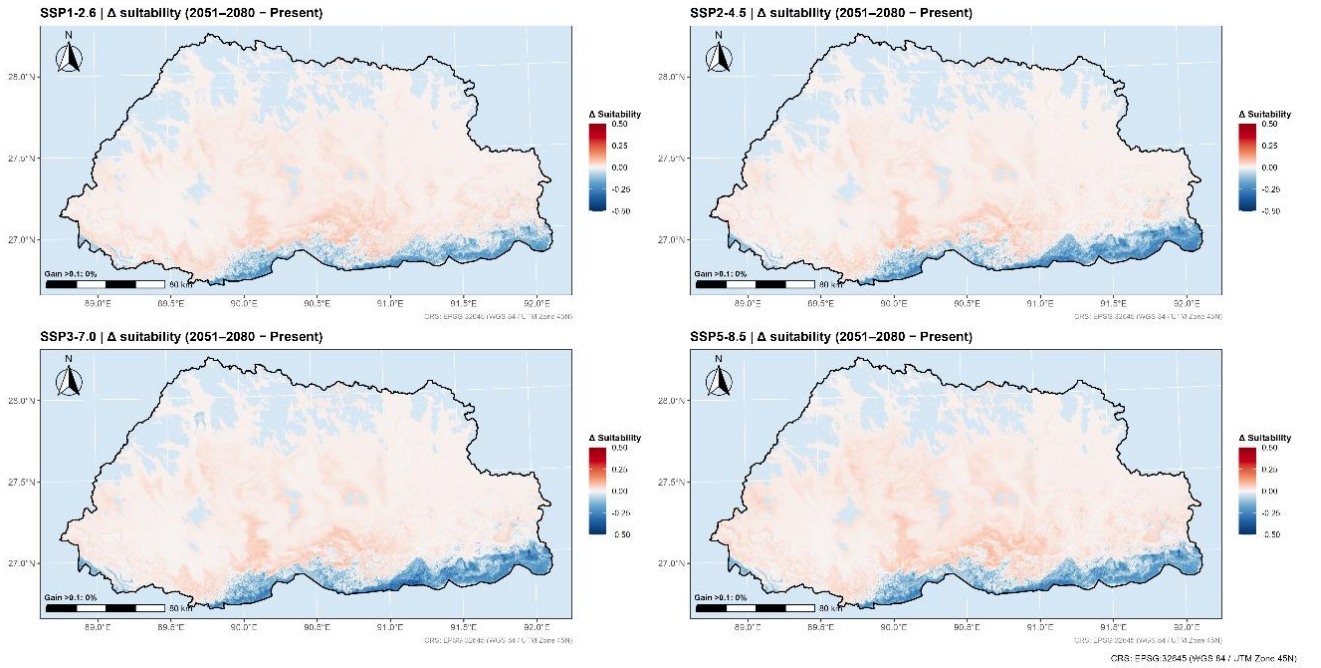

Figure S16b. Habitat change map 2051–2080.

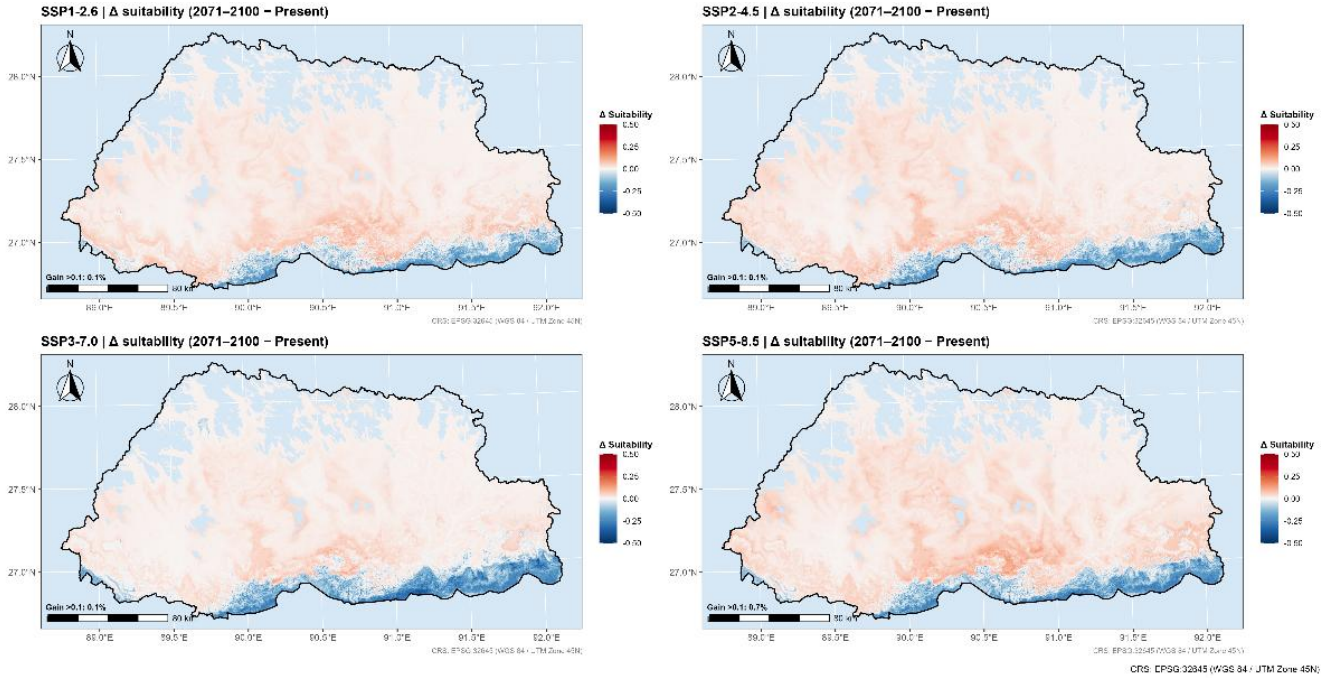

Figure S16c. Habitat change map 2071–2100.

Figure S17. Gain, loss, and persistence maps by time period. Spatial distribution of habitat gain (green), loss (red), and persistence (dark orange) relative to the present-day baseline for each future period: (a) 2021–2050; (b) 2051–2080; (c) 2071–2100 (mean across SSPs shown). Loss is concentrated at the southern thermal extreme; gain is concentrated in the submontane zone at 800–1,500 m. Persistence dominates across all periods (>4,200 km² under all scenarios).

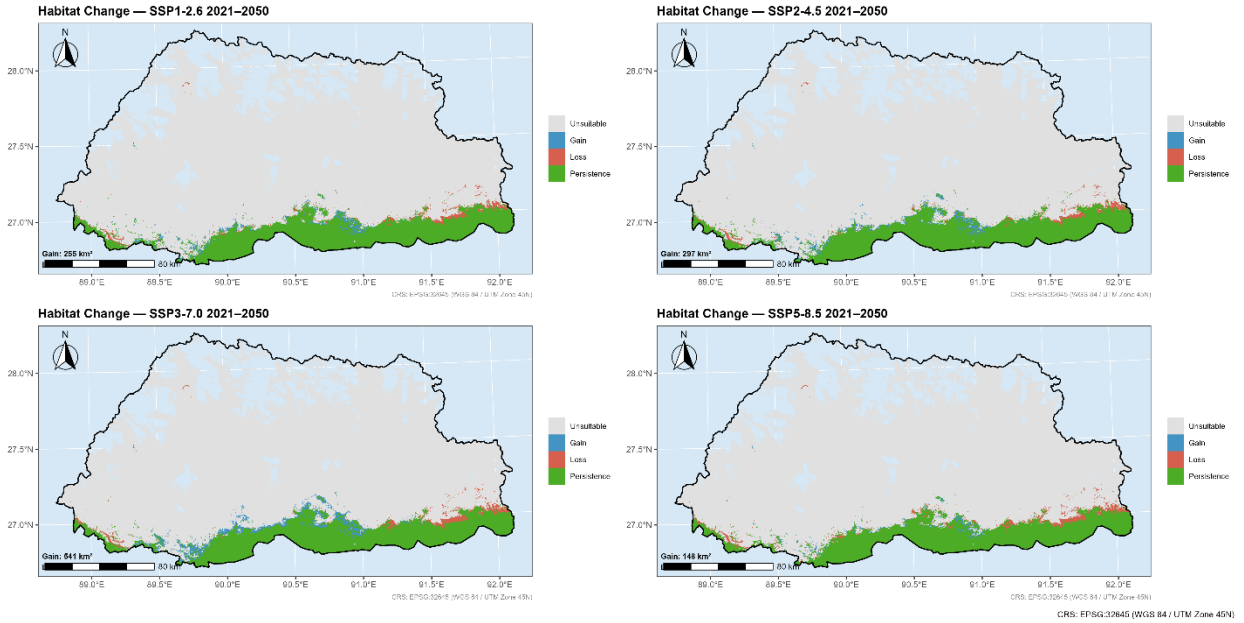

Figure S17a. Gain, loss, persistence 2021–2050.

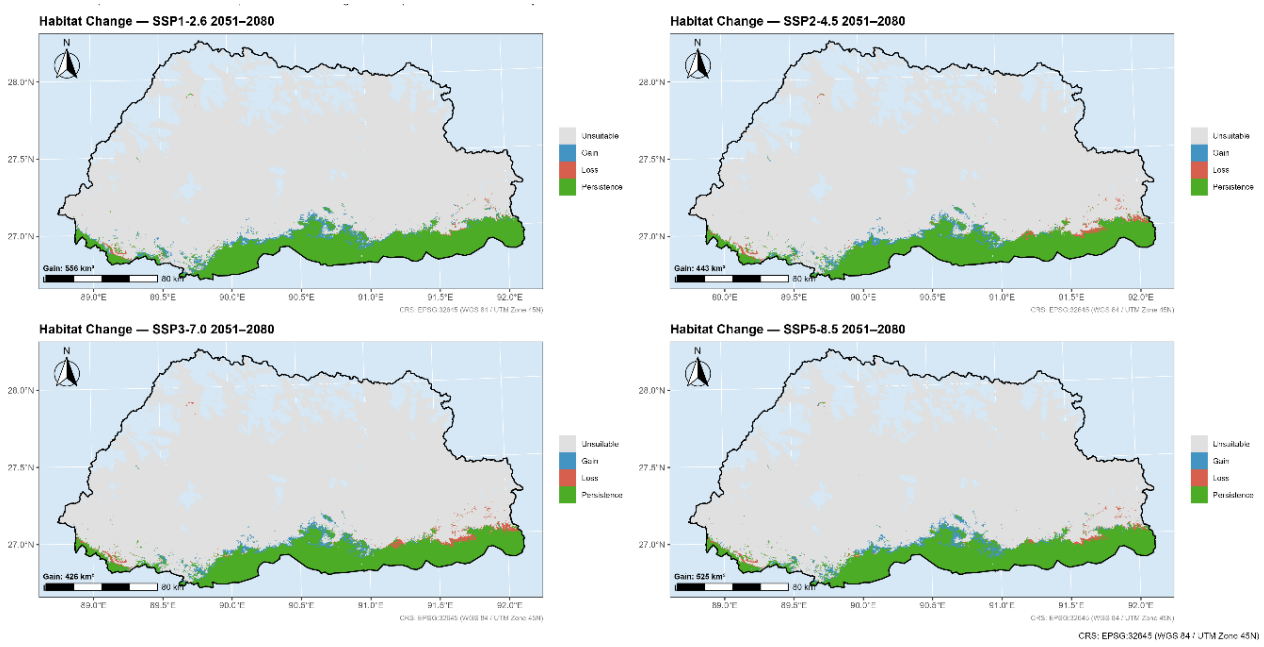

Figure S17b. Gain, loss, persistence 2051–2080.

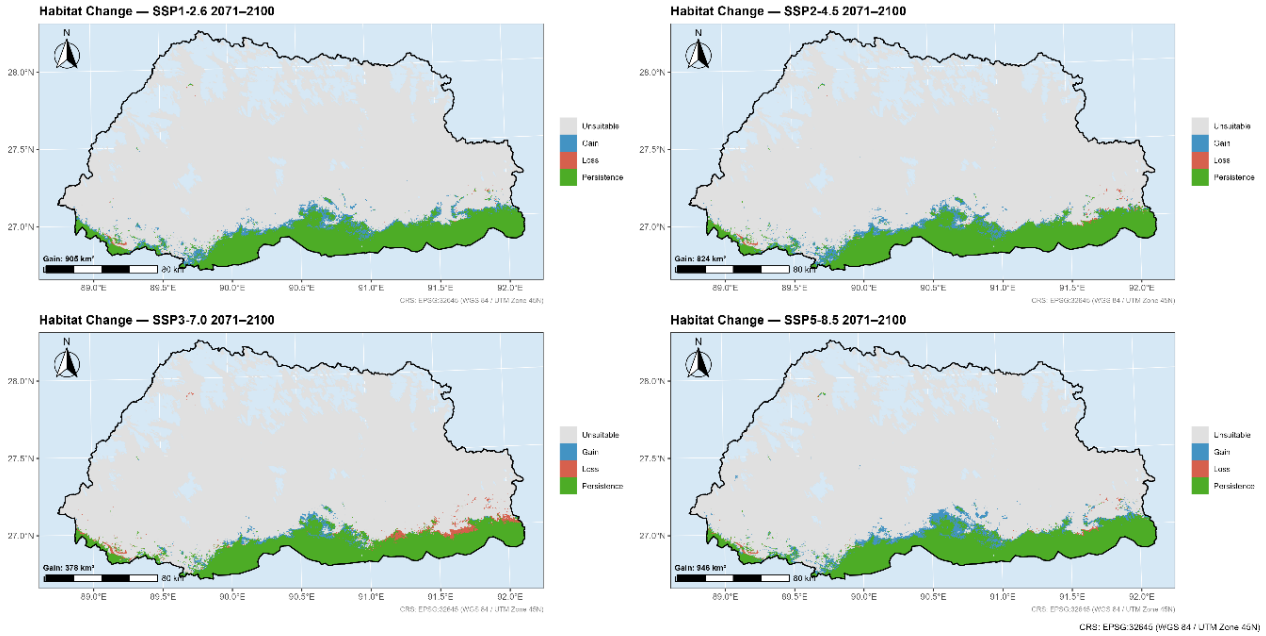

Figure S17c. Gain, loss, persistence 2071–2100.

Figure S18. Ensemble uncertainty maps by time period. Inter-GCM standard deviation of continuous suitability predictions for each future period under SSP5-8.5, the highest-uncertainty pathway. (a) 2021–2050 (mean SD = 0.016); (b) 2051–2080 (mean SD = 0.033); (c) 2071–2100 (mean SD = 0.042; 11.3% of pixels with high SD).

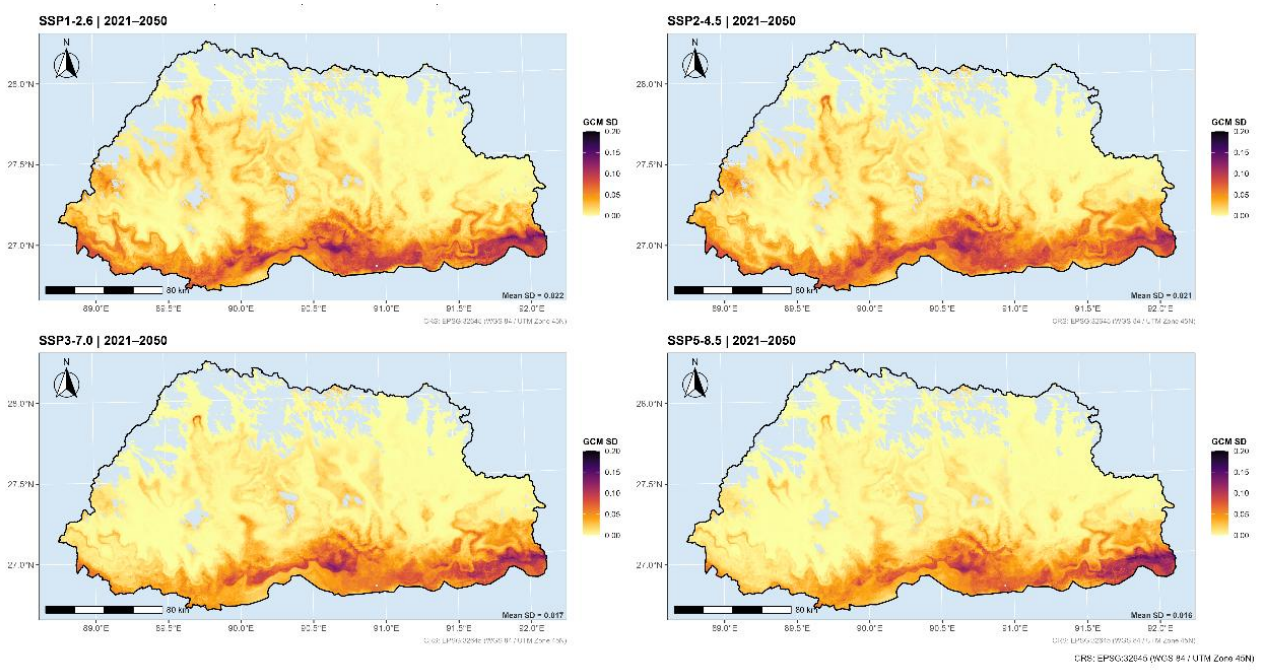

Figure S18a. Ensemble uncertainty 2021–2050.

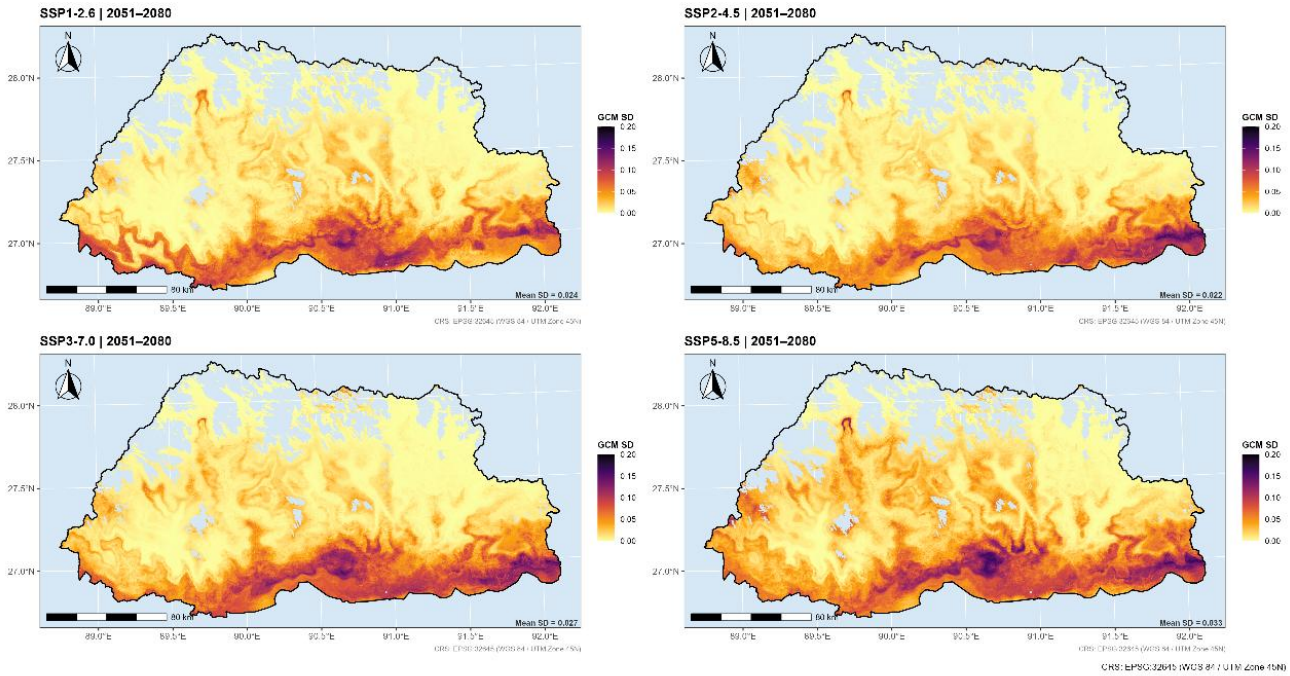

Figure S18b. Ensemble uncertainty 2051–2080.

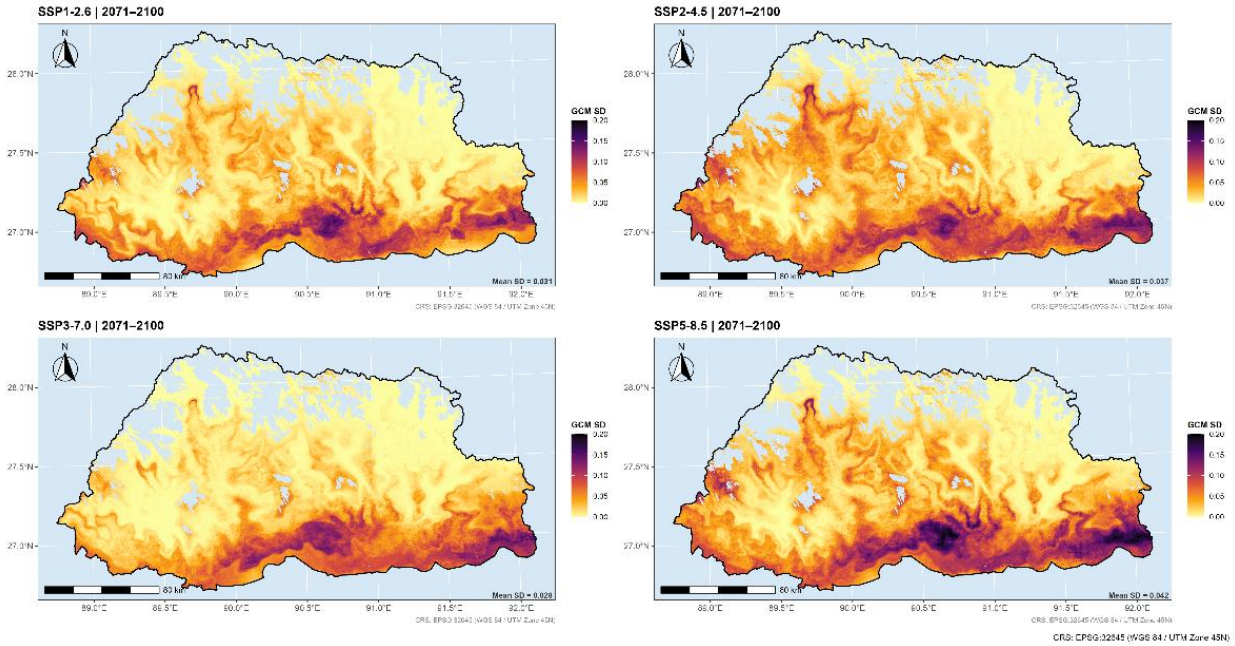

Figure S18c. Ensemble uncertainty 2071–2100.

Figure S19. Future human–elephant conflict risk — all scenarios. Projected mean conflict risk index under all four SSPs and three time periods. (a–c) Future conflict risk maps for SSP5-8.5 at 2021–2050, 2051–2080, and 2071–2100. (d–f) Corresponding conflict risk change maps (future minus present; red = increase, blue = decrease). All scenarios show risk escalation in the southern belt Dzongkhags.

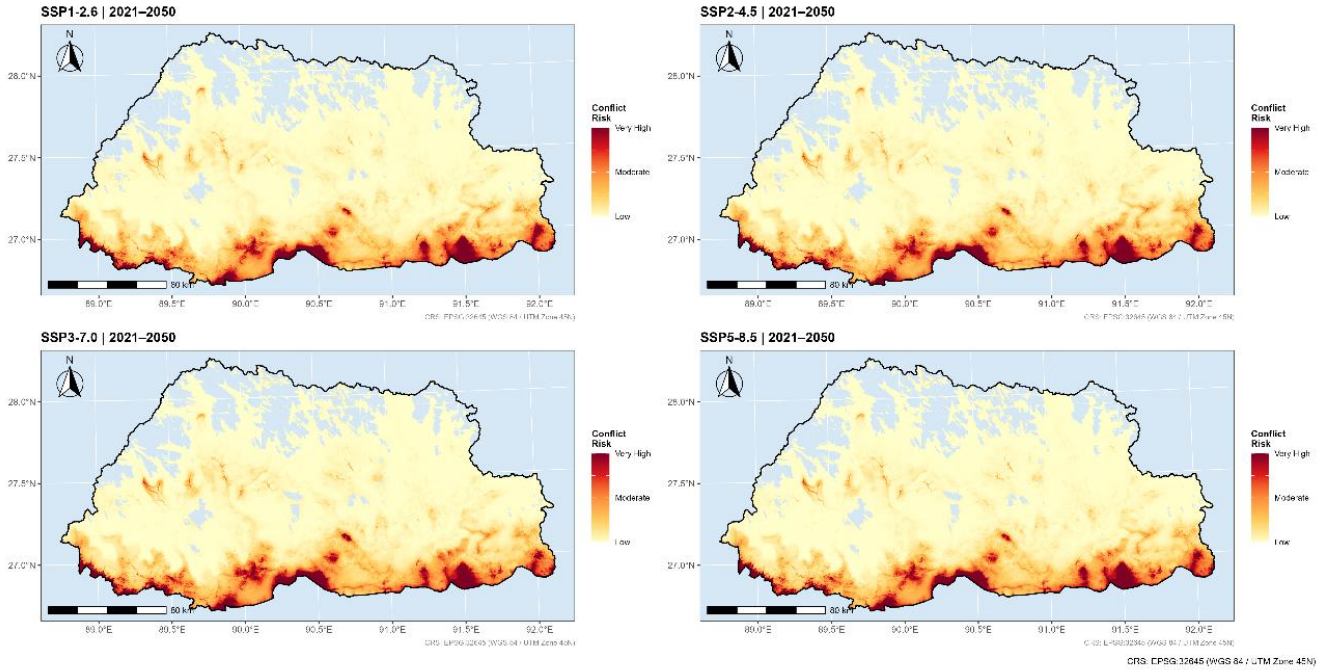

Figure S19a. Future conflict risk 2021–2050.

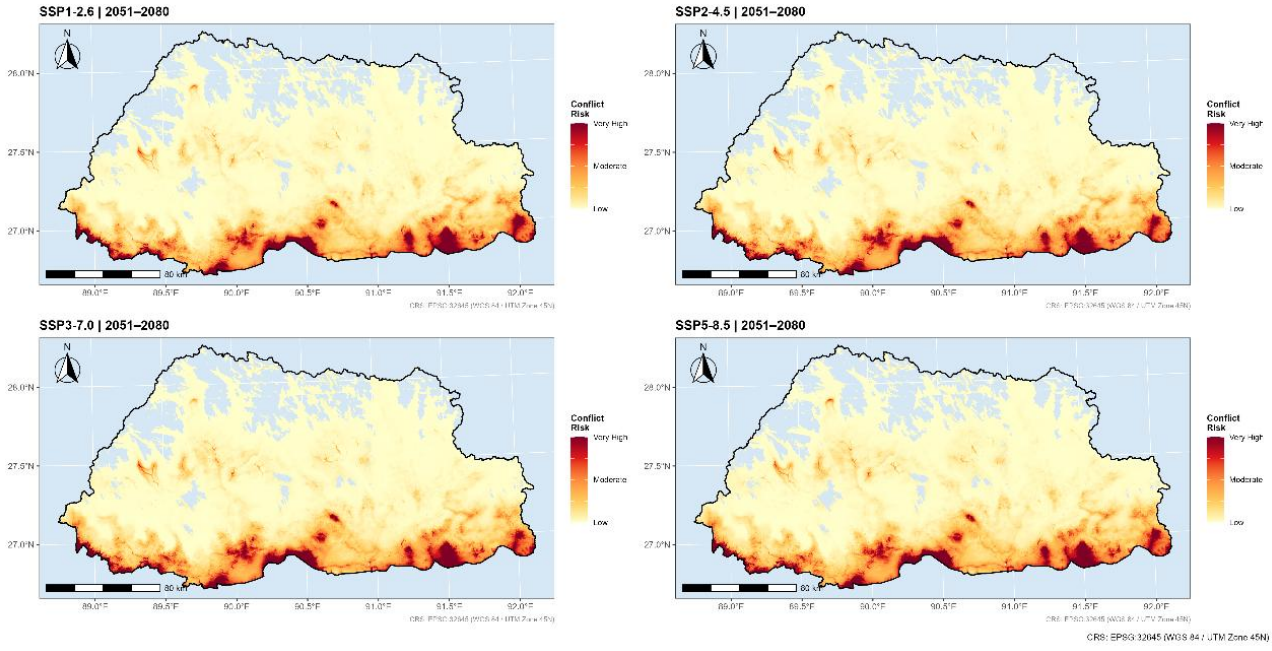

Figure S19b. Conflict risk change 2021–2050.

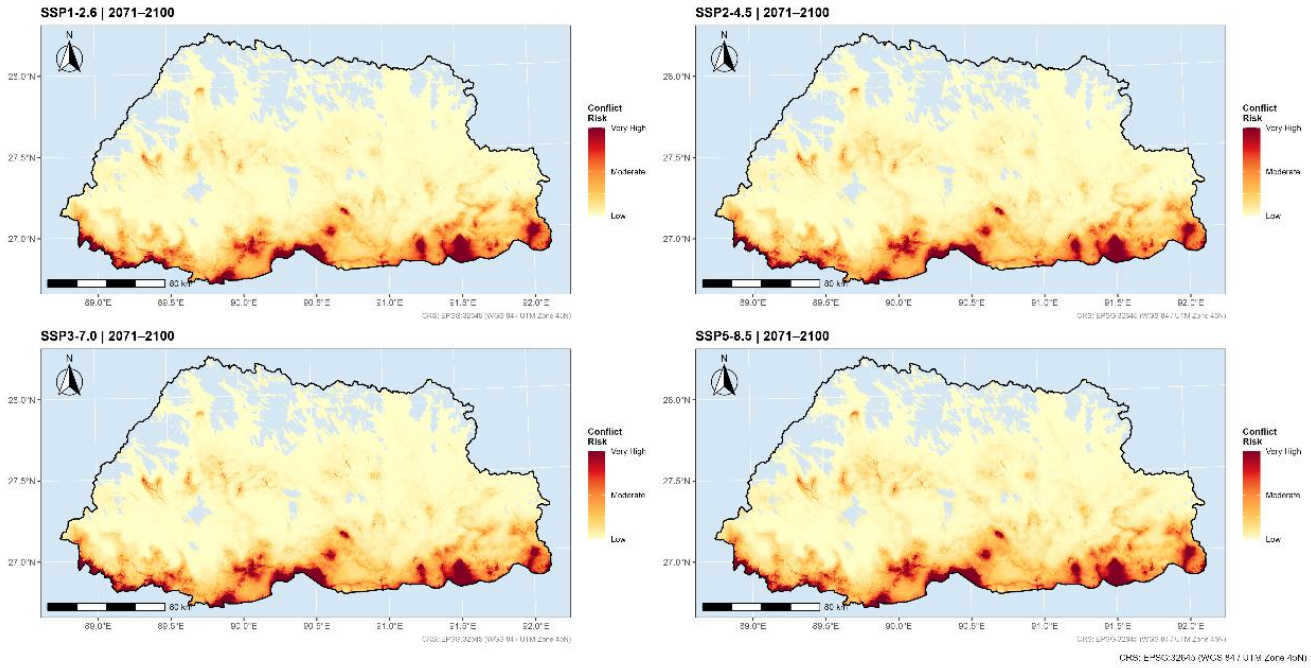

Figure S19c. Future conflict risk 2051–2080.

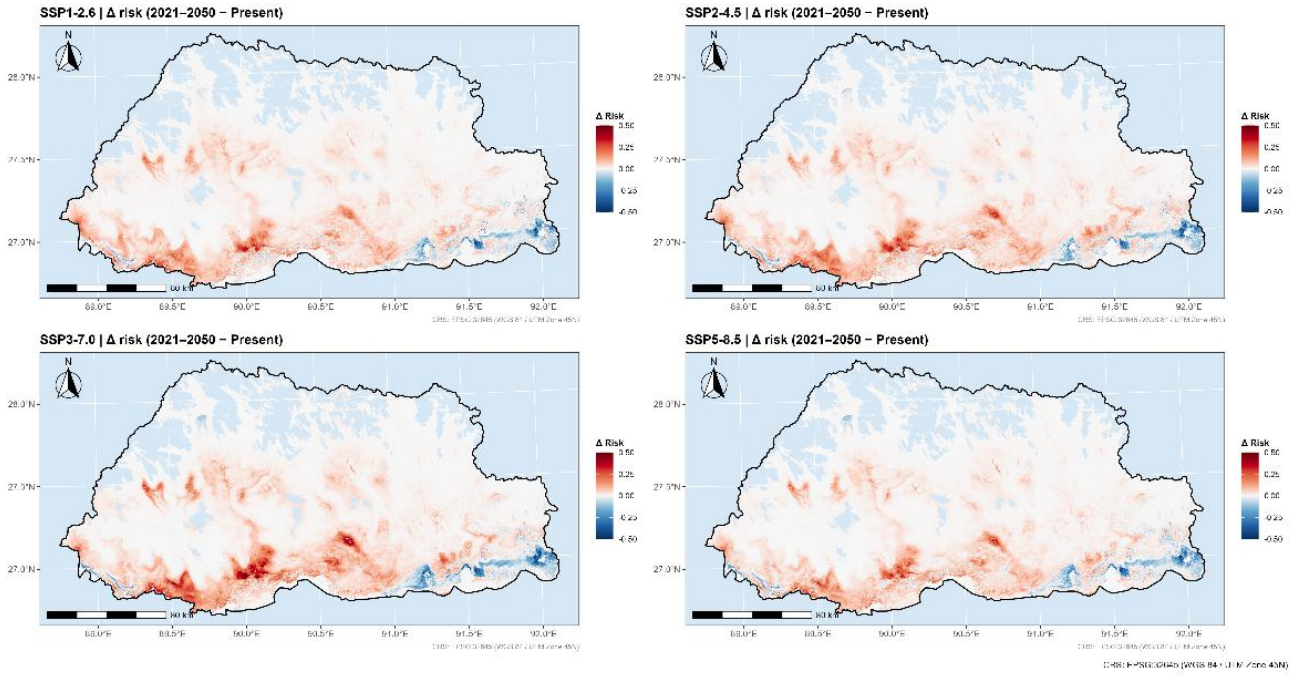

Figure S19d. Conflict risk change 2051–2080.

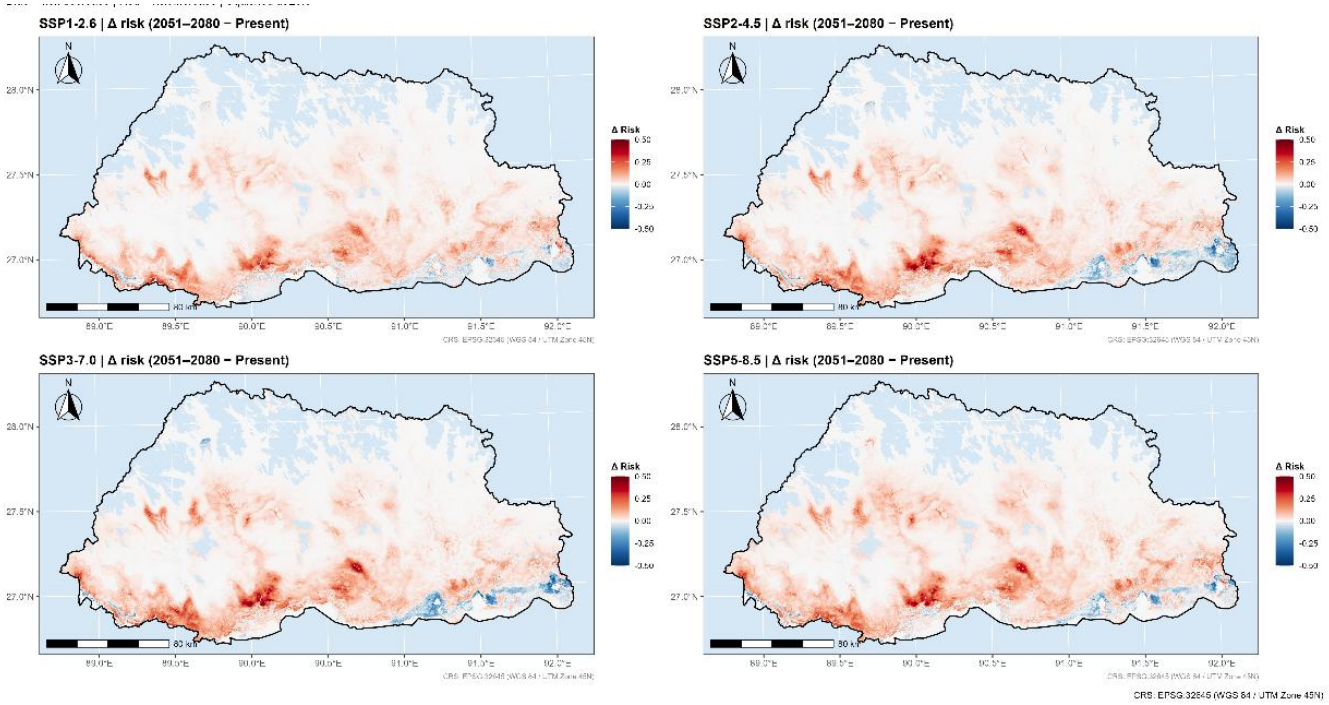

Figure S19e. Future conflict risk 2071–2100.

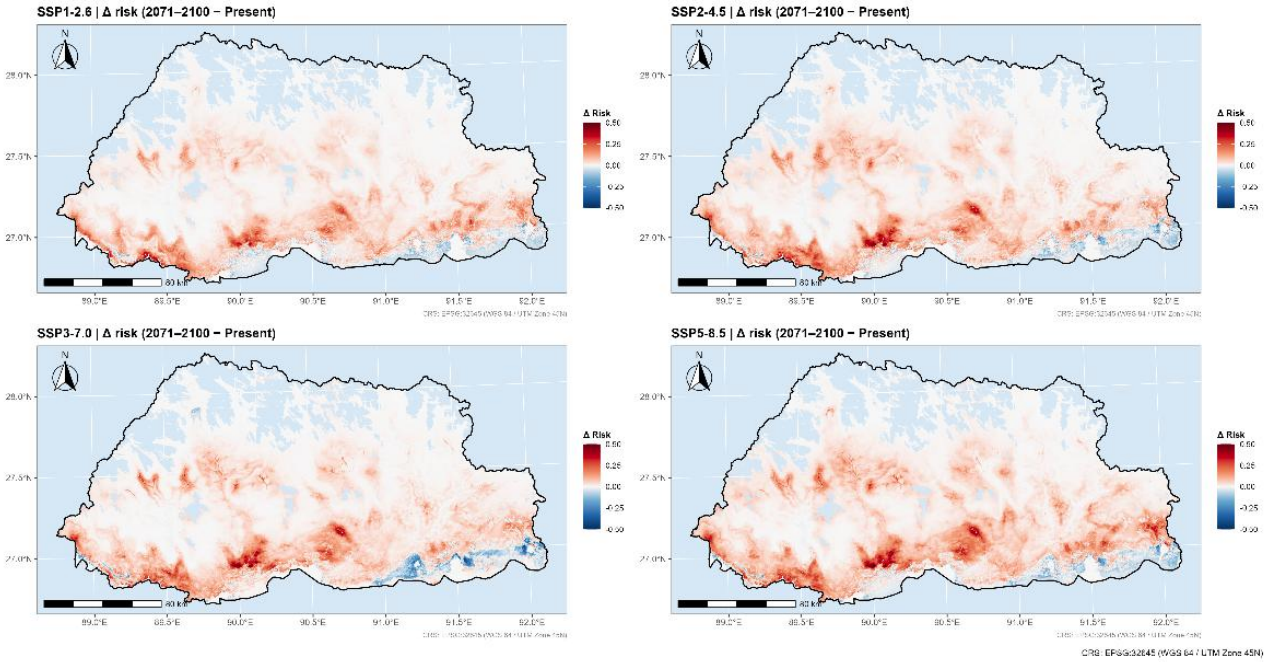

Figure S19f. Conflict risk change 2071–2100.

Figure S20. Spatial residual autocorrelogram (Moran's I). Moran's I of out-of-fold residuals as a function of spatial lag distance (km) for each of the four algorithms. Values close to zero across all distances indicate minimal residual spatial autocorrelation following spatially blocked cross-validation. All algorithms show Moran's I < 0.22 at the first distance class, confirming effective control of spatial autocorrelation.

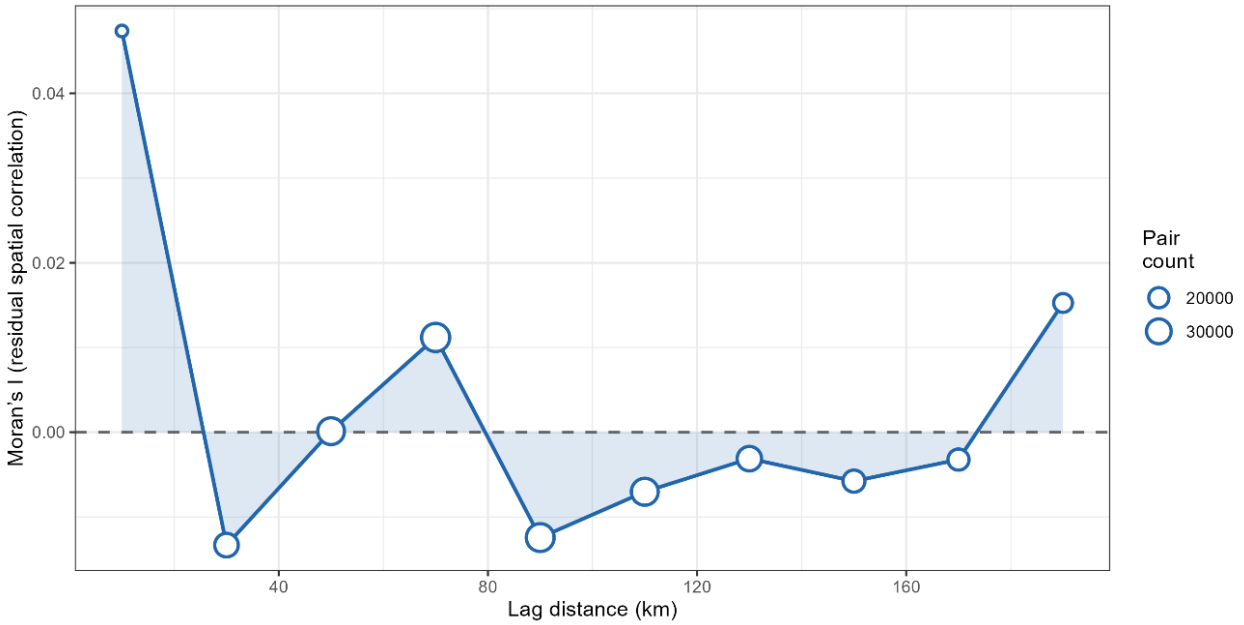

Figure S21. MESS extrapolation risk map — GCM-mean, SSP5-8.5, 2071–2100. Multivariate Environmental Similarity Surface (MESS; Elith et al., 2010) showing the mean extrapolation risk across 8 GCMs for the highest-emission, end-century scenario (SSP5-8.5, 2071–2100). Negative MESS values (red) indicate grid cells where projected climate falls outside the calibration climate space (1986–2015). Only 0.11% of pixels show MESS < 0 under this scenario — the maximum across all 12 SSP × period combinations — confirming that novel-climate extrapolation is not a meaningful source of uncertainty in these projections. White areas are fully within the training climate envelope.

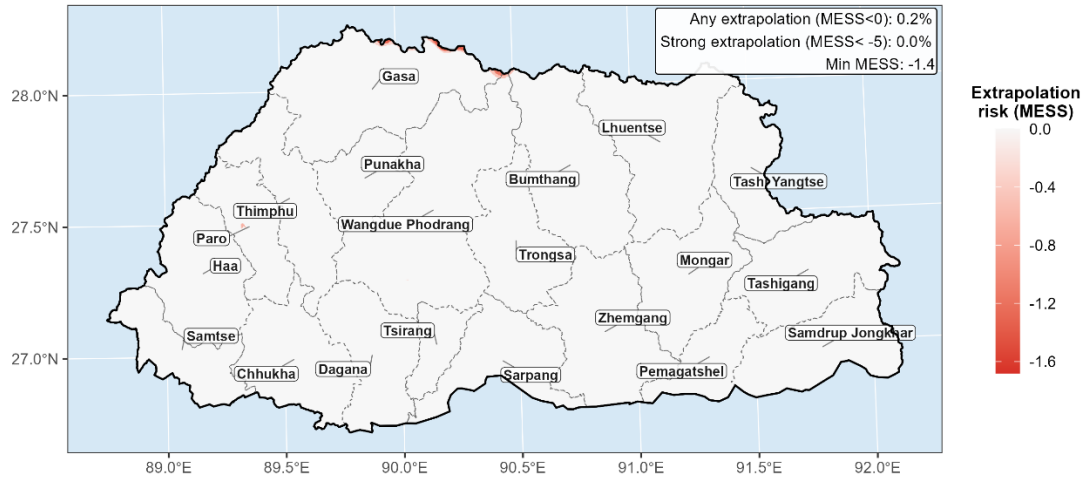

Supplementary Appendix S5: Supplementary Tables

Table S1. Full predictor list: all 35 candidate predictors, retained/removed status, and removal reason.

Predictor	Category	Status	Removal reason
human_footprint	Anthropogenic	Selected	-
BIO05	Climate (BIO)	Selected	-
BIO14	Climate (BIO)	Selected	-
BIO15	Climate (BIO)	Selected	-
BIO18	Climate (BIO)	Selected	-
BIO01	Climate (BIO)	Removed	Correlated (r=1.00) with BIO10
BIO02	Climate (BIO)	Removed	VIF 526.84 > 10.00
BIO03	Climate (BIO)	Removed	VIF 173.44 > 10.00
BIO04	Climate (BIO)	Removed	VIF 18.96 > 10.00
BIO06	Climate (BIO)	Removed	Correlated (r=0.96) with BIO05
BIO07	Climate (BIO)	Removed	VIF 356.03 > 10.00
BIO08	Climate (BIO)	Removed	Correlated (r=1.00) with BIO05
BIO09	Climate (BIO)	Removed	Correlated (r=0.98) with BIO05
BIO10	Climate (BIO)	Removed	Correlated (r=1.00) with BIO05
BIO11	Climate (BIO)	Removed	Correlated (r=0.99) with BIO10
BIO12	Climate (BIO)	Removed	Correlated (r=0.99) with BIO13
BIO13	Climate (BIO)	Removed	Correlated (r=0.99) with BIO18
BIO16	Climate (BIO)	Removed	Correlated (r=0.99) with BIO13
BIO17	Climate (BIO)	Removed	Correlated (r=0.97) with BIO14
BIO19	Climate (BIO)	Removed	Correlated (r=0.88) with BIO14
dist_to_major_rivers	Distance	Selected	-
dist_to_private_land	Distance	Selected	-
dist_to_protected_areas	Distance	Selected	-
dist_to_settlements	Distance	Selected	-
dist_to_streams	Distance	Selected	-
dist_to_water_sources	Distance	Selected	-
Aspect	Topography	Selected	-
Slope	Topography	Selected	-
Tri	Topography	Selected	-
Elevation	Topography	Removed	Correlated (r=-0.98) with BIO05
dynamicworld_prob	Vegetation/LULC	Selected	-
Evi	Vegetation/LULC	Selected	-
Landcover	Vegetation/LULC	Selected	-
Ndvi	Vegetation/LULC	Removed	Correlated (r=0.86) with dynamicworld_prob

Table S2. Environmental predictor statistics at presence and absence stations, with Cohen's d effect sizes.

Predictor	Category	Presence mean	Presence SD	Absence mean	Absence SD	Mean difference	Cohen's d
human_footprint	Anthropogenic	544.629	282.039	483.794	258.668	60.835	0.23
BIO05	Climate (BIO)	28.201	2.848	21.319	4.843	6.882	1.54
BIO14	Climate (BIO)	12.469	4.525	6.061	3.823	6.408	1.60
BIO15	Climate (BIO)	102.445	7.187	95.058	5.971	7.387	1.18
BIO18	Climate (BIO)	2085.787	676.868	1032.549	500.724	1053.237	1.93
dist_to_major_rivers	Distance	6519.481	5154.567	3391.774	2976.580	3127.707	0.87
dist_to_private_land	Distance	2645.830	2542.777	2574.295	2618.088	71.535	0.03
dist_to_protected_areas	Distance	2285.917	5936.335	6513.210	9550.200	-4227.293	-0.48
dist_to_settlements	Distance	13763.555	8035.989	11206.468	6760.700	2557.087	0.36
dist_to_streams	Distance	534.702	487.960	755.932	506.342	-221.231	-0.44
dist_to_water_sources	Distance	3480.260	3063.511	2745.073	2560.563	735.187	0.27
Aspect	Topography	175.868	79.379	179.225	89.524	-3.357	-0.04
Slope	Topography	9.857	6.434	15.476	7.696	-5.620	-0.76
Tri	Topography	47.338	24.836	73.138	22.991	-25.801	-1.10
dynamicworld_prob	Vegetation/LULC	0.675	0.061	0.658	0.076	0.017	0.23
Evi	Vegetation/LULC	0.421	0.046	0.351	0.084	0.070	0.91
landcover	Vegetation/LULC	0.944	0.230	0.918	0.604	0.027	0.05

Table S3. Multi-algorithm variable importance: normalised importance (%) for all 17 retained predictors.

Algorithm	Predictor	Category	Relative importance (%)
BRT	BIO18	Climate (BIO)	100
BRT	dist_to_protected_areas	Distance	22.7
BRT	BIO14	Climate (BIO)	20.6
BRT	BIO05	Climate (BIO)	17.4
BRT	Tri	Topography	13.6
BRT	BIO15	Climate (BIO)	13.6
BRT	dist_to_major_rivers	Distance	11
BRT	dynamicworld_prob	Vegetation/LULC	6.5
BRT	dist_to_private_land	Distance	6
BRT	slope	Topography	3.3
BRT	aspect	Topography	3.2
BRT	Evi	Vegetation/LULC	2.8
BRT	dist_to_water_sources	Distance	2.5
BRT	human_footprint	Anthropogenic	2.3
BRT	dist_to_settlements	Distance	1.6
BRT	dist_to_streams	Distance	0.9
BRT	landcover	Vegetation/LULC	0.3
GLM	BIO14	Climate (BIO)	100
GLM	BIO15	Climate (BIO)	95.7
GLM	BIO05	Climate (BIO)	44.4
GLM	BIO18	Climate (BIO)	42.4
GLM	dist_to_protected_areas	Distance	27.1
GLM	Tri	Topography	25.8
GLM	dist_to_water_sources	Distance	24.8
GLM	landcover	Vegetation/LULC	13.9
GLM	dist_to_major_rivers	Distance	13.6
GLM	dynamicworld_prob	Vegetation/LULC	13.5
GLM	dist_to_settlements	Distance	11.5
GLM	Evi	Vegetation/LULC	5.5
GLM	dist_to_streams	Distance	5.4
GLM	human_footprint	Anthropogenic	0.5
GLM	dist_to_private_land	Distance	0.3
GLM	aspect	Topography	0.2
GLM	slope	Topography	0.1

Algorithm	Predictor	Category	Relative importance (%)
MaxEnt	BIO18.contribution	Climate (BIO)	100
MaxEnt	slope.contribution	Topography	29.4
MaxEnt	dist_to_protected_areas.contribution	Topography	15.5
MaxEnt	BIO05.contribution	Climate (BIO)	10
MaxEnt	BIO14.contribution	Climate (BIO)	9.6
MaxEnt	BIO15.contribution	Climate (BIO)	5.2
MaxEnt	dynamicworld_prob.contribution	Vegetation/LULC	3.3
MaxEnt	dist_to_private_land.contribution	Topography	3.1
MaxEnt	tri.contribution	Topography	2.7
MaxEnt	dist_to_settlements.contribution	Topography	2.5
MaxEnt	dist_to_major_rivers.contribution	Topography	2.3
MaxEnt	dist_to_streams.contribution	Topography	1.6
MaxEnt	aspect.contribution	Topography	1.4
MaxEnt	evi.contribution	Vegetation/LULC	1
MaxEnt	landcover.contribution	Vegetation/LULC	1
MaxEnt	dist_to_water_sources.contribution	Topography	0.4
MaxEnt	human_footprint.contribution	Anthropogenic	0.1
RF	BIO18	Climate (BIO)	100
RF	BIO14	Climate (BIO)	64.9
RF	BIO05	Climate (BIO)	44.5
RF	BIO15	Climate (BIO)	34.2
RF	Tri	Topography	26.9
RF	dist_to_protected_areas	Distance	19.6
RF	dist_to_major_rivers	Distance	18.1
RF	dist_to_private_land	Distance	8.7
RF	Evi	Vegetation/LULC	8.3
RF	slope	Topography	7.1
RF	human_footprint	Anthropogenic	6.6
RF	dist_to_water_sources	Distance	6.4
RF	dist_to_settlements	Distance	5.5
RF	dynamicworld_prob	Vegetation/LULC	3.8
RF	dist_to_streams	Distance	2.4
RF	Aspect	Topography	2.3
RF	Landcover	Vegetation/LULC	0.3

Table S4. Algorithm hyperparameters and software details.

Algorithm	Package / engine	Key parameters	Seed controlled	Verification source
GLM	Stats	family = binomial, link = logit; forward stepwise AIC selection	Yes	E:_maximus_SDM_Project_v4\03_analysis\07_model_training.R
Random Forest	ranger	num.trees = 1000, mtry = 4 (floor(sqrt(17 predictors))), min.node.size = 1	Yes	E:_maximus_SDM_Project_v4\03_analysis\07_model_training.R
BRT	Gbm	n.trees = 1000, interaction.depth = 3, shrinkage = 0.01, bag.fraction = 0.75; OOB stopping	Yes	E:_maximus_SDM_Project_v4\03_analysis\07_model_training.R
MaxEnt	maxent.jar	betamultiplier = 1.5; feature classes used by model = hinge, product, linear, quadratic; output = cloglog	Yes	E:_maximus_SDM_Project_v4\04_outputs_20260326_104659_b990\02_models_full_maximus.html

Table S5a. Spatial cross-validation fold composition.

Fold	N presences	N absences	Presence:absence ratio
1	19	155	0.12
2	66	194	0.34
3	58	157	0.37
4	80	160	0.50
5	29	171	0.17

Table S5b. Per-fold AUC by algorithm.

Fold	AUC GLM	AUC RF	AUC BRT	AUC MaxEnt
1	0.956	0.988	0.989	0.988
2	0.897	0.928	0.905	0.927
3	0.927	0.939	0.944	0.942
4	0.877	0.903	0.897	0.904
5	0.956	0.984	0.981	0.985

Table S6. Threshold sensitivity analysis - habitat area under alternative ensemble suitability thresholds.

Threshold	% of Bhutan suitable	Area (km2)	Notes
0.050	28.6%	9,439	
0.100	19.7%	6,486	
0.150	15.5%	5,112	
0.174	14.2%	4,670	Current threshold
0.200	13.0%	4,303	
0.250	11.4%	3,768	
0.300	10.2%	3,349	
0.400	8.0%	2,626	
0.500	5.9%	1,938	

At the selected threshold (0.174), the present-day ensemble suitability surface classified 4,670 km² (14.2% of Bhutan) as suitable habitat.

Table S7. Suitability within individual protected areas - all 19 PA units.

Rank	PA name	Area (km^2)	Mean suitability	SD suitability	% suitable	Suitable area (km^2)
1	Biological Corridor 5	218.7	0.743	0.072	100.0%	218.7
2	Phibsoo Wildlife Sanctuary	297.5	0.720	0.147	100.0%	297.5
3	Jomotsangkha Wildlife Sanctuary	372.4	0.635	0.112	100.0%	372.4
4	Royal Manas National Park	1079.6	0.390	0.244	77.5%	837.1
5	Biological Corridor 3	443.8	0.239	0.188	47.6%	211.2
6	Biological Corridor 6	249.6	0.191	0.180	39.4%	98.4
7	Jigme Singye Wangchuck National Park	1660.3	0.032	0.044	2.6%	43.7
8	Biological Corridor 4	603.4	0.030	0.032	0.7%	4.5
9	Royal Botanical Park	101.7	0.030	0.016	0.0%	0.0
10	Jigme Khesar Strick Nature	634.6	0.020	0.014	0.0%	0.0

Rank	PA name	Area (km^2)	Mean suitability	SD suitability	% suitable	Suitable area (km^2)
	Reserve					
11	Biological Corridor 2	306.6	0.018	0.010	0.0%	0.0
12	Biological Corridor 8	596.9	0.016	0.008	0.0%	0.0
13	Jigme Dorji Wangchuch National Park	2064.3	0.016	0.020	0.2%	4.3
14	Wangchuck Centennial National Park	2899.4	0.014	0.009	0.0%	0.0
15	Sakteng Wildlife Sanctuary	725.4	0.013	0.012	0.0%	0.1
16	Biological Corridor 7	461.8	0.012	0.006	0.0%	0.0
17	Phrumsengla National Park	902.9	0.012	0.007	0.0%	0.0
18	Biological Corridor 1	221.4	0.009	0.004	0.0%	0.0
19	Bumdeling Wildlife Sanctuary	976.8	0.009	0.005	0.0%	0.0

Per-unit suitable areas are not additive because corridor and protected-area polygons overlap. Protected-area coverage was therefore estimated from the combined protected-area network on the common 250 m analysis grid. At the binary suitability threshold of 0.174, 2,003.8 km² of present-day suitable habitat occurred inside the protected-area network.

Table S8. GCM reliability ranking - all 8 GCMs.

Rank	GCM	Institution	Intra-algorithm SD	Ensemble deviation	Composite score
1	INM-CM5-0	Institute for Numerical Mathematics (Russia)	0.0647	0.0157	0.840
2	CNRM-CM6-1	Meteo-France/CNRM (France)	0.0472	0.0307	0.804
3	MIROC6	JAMSTEC/NIES/AORI (Japan)	0.0512	0.0288	0.796
4	MPI-ESM1-2-LR	Max Planck Institute (Germany)	0.0433	0.0362	0.771
5	CNRM-	Meteo-France/CNRM	0.0479	0.0336	0.767

Rank	GCM	Institution	Intra-algorithm SD	Ensemble deviation	Composite score
	ESM2-1	(France)			
6	INM-CM4-8	Institute for Numerical Mathematics (Russia)	0.0835	0.0270	0.575
7	ACCESS-CM2	CSIRO/ARCCSS (Australia)	0.0923	0.0407	0.356
8	MRI-ESM2-0	Meteorological Research Institute (Japan)	0.1104	0.0606	0.000

Note. The composite score was used only for diagnostic ranking; future SSP–period projections were calculated as simple arithmetic means across the 8 GCMs.

Table S9. Inter-GCM ensemble spread - mean and maximum standard deviation of continuous suitability scores across 8 GCMs, by SSP and period.

SSP	Period	Mean GCM SD	Median GCM SD	Max GCM SD	% pixels with high SD (>0.10)
SSP1-2.6	2021-2050	0.0215	0.0098	0.1686	1.5%
SSP1-2.6	2051-2080	0.0238	0.0101	0.1548	2.0%
SSP1-2.6	2071-2100	0.0306	0.0200	0.1763	4.2%
SSP2-4.5	2021-2050	0.0214	0.0089	0.1344	1.0%
SSP2-4.5	2051-2080	0.0224	0.0095	0.1754	2.5%
SSP2-4.5	2071-2100	0.0372	0.0294	0.1672	5.2%
SSP3-7.0	2021-2050	0.0174	0.0063	0.1539	1.0%
SSP3-7.0	2051-2080	0.0266	0.0117	0.1723	4.3%
SSP3-7.0	2071-2100	0.0282	0.0134	0.1731	5.2%
SSP5-8.5	2021-2050	0.0157	0.0041	0.1610	1.5%
SSP5-8.5	2051-2080	0.0327	0.0226	0.1809	4.6%
SSP5-8.5	2071-2100	0.0421	0.0290	0.2132	11.3%

Table S10. Individual GCM habitat area trajectories - percentage of Bhutan classified as suitable under each GCM x SSP x period combination.

GCM	Reliability score	SSP1-2.6 2021–2050	SSP1-2.6 2051–2080	SSP1-2.6 2071–2100	SSP2-4.5 2021–2050	SSP2-4.5 2051–2080	SSP2-4.5 2071–2100	SSP3-7.0 2021–2050	SSP3-7.0 2051–2080	SSP3-7.0 2071–2100	SSP5-8.5 2021–2050	SSP5-8.5 2051–2080	SSP5-8.5 2071–2100
ACCESS-CM2	0.356	18.8%	21.6%	22.9%	21.0%	19.1%	22.6%	19.5%	22.5%	25.7%	18.1%	23.1%	26.2%
CNRM-CM6-1	0.804	15.7%	20.4%	12.0%	15.6%	21.1%	15.5%	17.3%	19.3%	14.4%	14.6%	13.6%	10.5%
CNRM-ESM2-1	0.767	10.7%	12.9%	15.1%	11.0%	10.2%	11.9%	14.3%	8.7%	11.1%	10.3%	9.8%	10.3%
INM-CM4-8	0.575	10.8%	12.2%	11.7%	11.7%	14.0%	15.0%	17.4%	14.0%	15.5%	14.7%	15.2%	21.3%
INM-CM5-0	0.840	11.2%	12.0%	15.4%	10.6%	15.1%	11.5%	13.3%	12.8%	16.2%	12.4%	11.7%	16.7%

GCM	Reliability score	SSP1-2.6 2021–2050	SSP1-2.6 2051–2080	SSP1-2.6 2071–2100	SSP2-4.5 2021–2050	SSP2-4.5 2051–2080	SSP2-4.5 2071–2100	SSP3-7.0 2021–2050	SSP3-7.0 2051–2080	SSP3-7.0 2071–2100	SSP5-8.5 2021–2050	SSP5-8.5 2051–2080	SSP5-8.5 2071–2100
MIROC6	0.796	13.0%	11.6%	15.9%	13.8%	12.0%	17.8%	13.0%	12.6%	9.6%	12.0%	11.5%	12.2%
MPI-ESM1-2-LR	0.771	13.3%	18.5%	16.6%	12.6%	10.7%	10.4%	11.5%	8.4%	7.7%	12.1%	12.7%	9.3%
MRI-ESM2-0	0.000	18.9%	15.1%	25.7%	18.1%	15.5%	31.9%	10.3%	16.9%	14.5%	10.2%	26.5%	30.7%

Table S11. Present-day human-elephant conflict risk zones - area and percentage of Bhutan.

Risk class	Risk score range	Area (km2)	% of Bhutan
Low	Risk ≤ 0.040	13,189	40%
Moderate	0.040 – 0.069	8,243	25%
High	0.069 – 0.164	6,595	20%
Very High	> 0.164	4,946	15%

Risk was derived from normalised ensemble suitability multiplied by a human-pressure surface combining human footprint and settlement proximity, then re-normalised to [0,1]. The cleaned conflict archive contained 151 incident records.

Table S12. Future mean human-elephant conflict risk index by SSP and time period.

SSP	Period	Mean conflict risk	Change from present	% change
Present	Baseline	0.103		
SSP1-2.6	2021-2050	0.118	+0.015	+14.6%
SSP1-2.6	2051-2080	0.122	+0.019	+18.4%
SSP1-2.6	2071-2100	0.127	+0.024	+23.3%
SSP2-4.5	2021-2050	0.120	+0.017	+16.5%
SSP2-4.5	2051-2080	0.124	+0.021	+20.4%
SSP2-4.5	2071-2100	0.132	+0.029	+28.2%
SSP3-7.0	2021-2050	0.124	+0.021	+20.4%
SSP3-7.0	2051-2080	0.126	+0.023	+22.3%
SSP3-7.0	2071-2100	0.129	+0.026	+25.2%
SSP5-8.5	2021-2050	0.116	+0.013	+12.6%
SSP5-8.5	2051-2080	0.130	+0.027	+26.2%
SSP5-8.5	2071-2100	0.140	+0.037	+35.9%

Table S13. Habitat suitability by Dzongkhag (administrative district) - all 20 Dzongkhags.

Rank	Dzongkhag	Code	Total area (km^2)	Suitable area (km^2)	% suitable	Mean suitability	Max suitability
1	Samdrup Jongkhar	11	1875.3	1301.3	69.4%	0.390	0.913
2	Pemagatshel	9	1024.4	602.2	58.8%	0.331	0.960
3	Sarpang	13	1654.9	966.9	58.4%	0.320	0.969
4	Zhemgang	20	2395.3	778.8	32.5%	0.163	0.951
5	Dagana	3	1693.1	446.6	26.4%	0.150	0.948
6	Tsirang	18	638.6	159.8	25.0%	0.147	0.793
7	Samtse	12	1295.2	262.2	20.2%	0.122	0.680
8	Chhukha	2	1861.8	115.4	6.2%	0.063	0.568
9	Tashigang	15	2182.1	10.4	0.5%	0.028	0.324
10	Mongar	7	1953.3	8.1	0.4%	0.021	0.503
11	Gasa	4	1312.0	4.3	0.3%	0.017	0.251
12	Paro	8	1016.1	0.6	0.1%	0.015	0.218
13	Bumthang	1	2078.0	0.0	0.0%	0.014	0.138
14	Haa	5	1637.3	0.6	0.0%	0.022	0.254
15	Lhuentse	6	2151.5	0.0	0.0%	0.012	0.090
16	Punakha	10	1057.8	0.0	0.0%	0.019	0.109
17	Thimphu	14	1058.4	0.0	0.0%	0.012	0.124
18	Tashi Yangtse	16	1133.2	0.0	0.0%	0.010	0.080
19	Trongsa	17	1699.3	0.1	0.0%	0.017	0.202
20	Wangdue Phodrang	19	3249.8	0.0	0.0%	0.016	0.118

District totals sum to 4,657.3 km² because district-level polygon aggregation and national grid-based thresholding are not perfectly identical operations.

Table S14. Occurrence data processing steps and record counts.

Processing step	Count	Notes
Operational input file	elephant_PA_data.csv	E:_maximus_SDM_Project_v4\01_data_raw\01_occurrences_PA_data.csv
Raw input records	1,089	Station-level presence-absence records
After coordinate validity QC	1,089	No invalid or zero-coordinate records were removed
Final presences	252	Exact-coordinate deduplication only; no additional thinning
Final absences	837	Exact-coordinate deduplication only; no pseudo-absence generation
Presence:absence ratio	1:3.32	

Processing step	Count	Notes
Presence stations inside PAs	160 (63.5%)	From station_zone_summary.csv
Absence stations inside PAs	354 (42.3%)	From station_zone_summary.csv
Mean suitability at presence stations	0.716	From station_zone_summary.csv
Mean suitability at absence stations	0.085	From station_zone_summary.csv

Table S15. MESS (Multivariate Environmental Similarity Surface) extrapolation fraction by SSP and time period.

SSP	Period	GCM-mean extrapolation fraction	% of pixels with MESS < 0
SSP1-2.6	2021-2050	0.001023	0.10%
SSP1-2.6	2051-2080	0.000915	0.09%
SSP1-2.6	2071-2100	0.001029	0.10%
SSP2-4.5	2021-2050	0.001130	0.11%
SSP2-4.5	2051-2080	0.001203	0.12%
SSP2-4.5	2071-2100	0.001086	0.11%
SSP3-7.0	2021-2050	0.001453	0.15%
SSP3-7.0	2051-2080	0.001965	0.20%
SSP3-7.0	2071-2100	0.001955	0.20%
SSP5-8.5	2021-2050	0.001071	0.11%
SSP5-8.5	2051-2080	0.001163	0.12%
SSP5-8.5	2071-2100	0.001127	0.11%
Maximum		0.001965	0.20%
Mean across all 12		0.001260	0.13%

The maximum GCM-mean extrapolation fraction occurred under SSP3-7.0, 2051-2080. Extrapolation remained low in all scenario means.

Table S16. ODMAP protocol compliance checklist (Zurell et al., 2020).

ODMAP section	Item	Reported	Location
O1	Modelling objective stated	Yes	Supplementary Appendix S1; manuscript Introduction
D1	Biodiversity data type documented	Yes	Supplementary Appendix S1; Methods 2.2
D4	Occurrence processing	Yes	Supplementary Appendix S1; Table S14

ODMAP section	Item	Reported	Location
	documented		
D6	Predictor variables documented	Yes	Methods 2.3; Table S1
M1	Algorithms documented	Yes	Methods 2.4; Table S4
M4	Ensembling documented	Yes	Methods 2.4 and 2.6
M5	Threshold derivation documented	Yes	Methods 2.4; Table S6
A1	Evaluation metrics documented	Yes	Methods 2.5; Table 1
A3	Extrapolation assessment documented	Yes	Methods 2.6; Table S15
A4	Uncertainty quantified	Yes	Methods 2.6; Table S9
P1	Present predictions documented	Yes	Results 3.3; Table 3
P2	Future predictions documented	Yes	Results 3.4; Table 2
P4	Gain/loss/persistence documented	Yes	Table 2
P5	Conservation overlays documented	Yes	Results 3.3-3.6; Tables 3, S7, S13, S18
–	Ensemble OOF evaluation row	No	Not computed in outputs
–	MaxEnt TSS on OOF probabilities	No	Not computable because OOF probabilities were outside the standard [0,1] range

Table S17. Niche similarity between present and future habitat suitability projections across SSPs and time periods.

Comparison	SSP	Period	Schoener's D	Hellinger's I
Present vs SSP1-2.6 2021–2050	SSP1-2.6	2021-2050	0.8601	0.9843
Present vs SSP1-2.6 2051–2080	SSP1-2.6	2051-2080	0.8573	0.9847
Present vs SSP1-2.6 2071–2100	SSP1-2.6	2071-2100	0.8400	0.9813
Present vs SSP2-	SSP2-4.5	2021-2050	0.8607	0.9845

Comparison	SSP	Period	Schoener's D	Hellinger's I
4.5 2021–2050				
Present vs SSP2-4.5 2051–2080	SSP2-4.5	2051-2080	0.8453	0.9816
Present vs SSP2-4.5 2071–2100	SSP2-4.5	2071-2100	0.8205	0.9760
Present vs SSP3-7.0 2021–2050	SSP3-7.0	2021-2050	0.8401	0.9799
Present vs SSP3-7.0 2051–2080	SSP3-7.0	2051-2080	0.8342	0.9789
Present vs SSP3-7.0 2071–2100	SSP3-7.0	2071-2100	0.8218	0.9758
Present vs SSP5-8.5 2021–2050	SSP5-8.5	2021-2050	0.8670	0.9851
Present vs SSP5-8.5 2051–2080	SSP5-8.5	2051-2080	0.8241	0.9767
Present vs SSP5-8.5 2071–2100	SSP5-8.5	2071-2100	0.7913	0.9684

Table S18. Refugia stability-class breakdown for Elephas maximus in Bhutan.

Refugia class	Definition	Area (km^2)	% of Bhutan	% within protected areas
Core refugia	Currently suitable and retained in all 12 future scenario means	4,160	12.6	46.4
High-stability refugia	Currently suitable and retained in >=75% of the 12 future scenario means (>=9/12)	4,356	13.2	45.4

References (Supplementary)

Brown, C. F., Brumby, S. P., Guzder-Williams, B., Birch, T., Hyde, S. B., Mazzariello, J., *et al.* (2022). Dynamic World, near real-time global 10 m land use land cover mapping. *Scientific Data*, *9*, 251. https://doi.org/10.1038/s41597-022-01307-4

Cohen, J. (1988). *Statistical power analysis for the behavioral sciences* (2nd ed.). Lawrence Erlbaum Associates.

Dorji, S., Stewart, S., Bajwa, A., Aziz, A., Shabbir, A., & Adkins, S. (2025). *High-resolution (250 m) historical and projected (CMIP6) air temperature and precipitation grids for Bhutan* (Version 1) [Data set]. CSIRO. https://doi.org/10.25919/pec2-hs50

Elith, J., Kearney, M., & Phillips, S. (2010). The art of modelling range-shifting species. *Methods in Ecology and Evolution, 1*(4), 330–342. https://doi.org/10.1111/j.2041-210X.2010.00036.x

Karger, D. N., Conrad, O., Böhner, J., Kawohl, T., Kreft, H., Soria-Auza, R. W., *et al.* (2017). Climatologies at high resolution for the earth's land surface areas. *Scientific Data, 4*, 170122. https://doi.org/10.1038/sdata.2017.122

Sanderson, B. M., Knutti, R., & Caldwell, P. (2015). A representative democracy to reduce interdependency in a multimodel ensemble. *Journal of Climate, 28*(13), 5171–5194. https://doi.org/10.1175/JCLI-D-14-00362.1

Wilson, M. F. J., O'Connell, B., Brown, C., Guinan, J. C., & Grehan, A. J. (2007). Multiscale terrain analysis of multibeam bathymetry data for habitat mapping on the continental slope. *Marine Geodesy*, *30*(1–2), 3–35. https://doi.org/10.1080/01490410701295962

Zurell, D., Franklin, J., König, C., Bouchet, P. J., Dormann, C. F., Elith, J., *et al.* (2020). A standard protocol for reporting species distribution models. *Ecography, 43*(9), 1261–1277. https://doi.org/10.1111/ecog.04960